An NMR Perspective on Enzyme Dynamics

David D. Boehr, H. Jane Dyson,* and Peter E. Wright*

Department of Molecular Biology, The Scripps Research Institute, 10550 North Torrey Pines Road, La Jolla, California 92037

Received March 20, 2006

Contents

1. Introduction

1.1. The Case for Dynamics

Enzyme catalysis is an inherently dynamic process. Binding and release of ligands is often accompanied by conformational changes, both subtle and dramatic (reviewed more extensively in refs 1−4), and these conformational changes may be rate-limiting in the overall reaction scheme, for example in dihydrofolate reductase (DHFR),[5] triosephosphate isomerase (TIM),[6,7] and protein kinase A.[8] The catalytic step itself, by its very nature, is dynamic. Atomic fluctuations along the reaction coordinate lead to bonds being broken and new ones being formed. Binding of substrate can lead to the repositioning of catalytic groups, effectively bridging the dynamic processes of substrate binding and catalysis.[2,9] Protein vibrations and motions within the Michaelis complex itself have been hypothesized to couple to the reaction coordinate, supplying a direct link between protein dynamics and enzyme function (reviewed in refs 10−18).

Although intuitively we understand that proteins, and enzymes in particular, are dynamic molecules, the overwhelming view that emerges from structural biology is static. Protein structures from X-ray crystallography and NMR have provided important insight into the form and function of enzymes, yet they give only brief snapshots into the life of a protein. Static protein structures show only the lowest energy or "ground-state" conformation, and function may be dependent on brief excursions to higher energy conformations of the enzyme and its substrates.[19−22] Structural genomics[23−25] is increasing the number of snapshots available, but relevant dynamic information remains limited.[16]

The connections between structure, dynamics, and function have practical importance. If dynamics has consequences for function, then understanding dynamics is critical for both protein and ligand design. It will not only be necessary to position the correct catalytic groups in an engineered enzyme, but for full efficiency it will also be necessary to engineer the relevant dynamic modes into the protein of interest. This is illustrated by catalytic antibodies, which are selected to bind tightly to transition-state analogues but do not yet approach the efficiency of natural enzymes.[26] This may be due to our inability to properly mimic a "transition state", or it may be related to the dynamic information we have not selected.[26,27] Enzyme catalysis involves chemical transformation, binding of substrates, and release of products, and the dynamic processes that tie these events together may not be fully appreciated or captured in the selection process. There is also growing evidence that dynamics may be important in nonbiological catalysts (see, e.g., refs 28−30).

Protein dynamics is also critical for ligand or inhibitor binding. Many enzymes are key pharmacological targets, and the wealth of protein structural information has provided the foundation for many drug discovery programs. It has become apparent, however, that flexibility is key to ligand/target recognition, and this has been difficult to predict based on structural information alone. Protein flexibility may lead to unexpected ligand-binding orientations or sites and may be responsible for selectivity between related receptors.[31] Protein dynamics also has a more subtle impact on ligand binding. The Gibbs free energy (ΔG) determines the affinity between protein and inhibitor, and while the enthalpy component (ΔH) is comparatively well-understood, entropy changes (ΔS) are much more difficult to model.[32,33] Enthalpy and entropy

* Corresponding authors. Telephone: 858 784 9721 (P.E.W.); 858 784 2223 (H.J.D.). Fax: 858 784 9822. E-mail: wright@scripps.edu; dyson@scripps.edu.

10.1021/cr050312q CCC: $59.00
Published on Web 07/26/2006

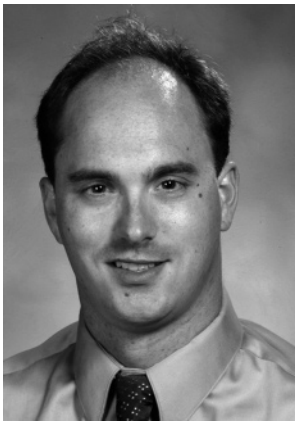

David Boehr received a B.Sc. degree from the University of Lethbridge (Lethbridge, Alberta, Canada) in 1997 and a Ph.D. from McMaster University (Hamilton, Ontario, Canada) in 2003 under the supervision of Gerard D. Wright with scholarship support from the Natural Sciences and Engineering Research Council (NSERC) of Canada. For his Ph.D. research, he used enzyme kinetics and other traditional enzymatic techniques to study the catalytic mechanisms of various antibiotic modifying enzymes toward the goal of developing novel inhibitor strategies to overcome antibiotic resistance. He is presently a Canadian Institutes of Health Research postdoctoral fellow at the Scripps Research Institute under the direction of Peter Wright. His current research interests include the interplay of dynamics in the function of enzymes, blending both traditional enzymatic techniques and newer NMR spin relaxation methodologies.

Jane Dyson received the degree of B.Sc. (honors) from the University of Sydney in 1973 and a Ph.D. from the University of Sydney in 1977, under the direction of James Beattie. She was a postdoctoral fellow at Massachusetts Institute of Technology under the direction of Paul Schimmel from 1977 to 1978, and she held a Damon Runyon–Walter Winchell postdoctoral award. She was appointed as a Lecturer in Chemistry at the University of New South Wales in 1979, and she joined the Scripps Research Institute in 1984, where she is presently a Professor. Her research interests are in the conformation of peptides, protein folding and dynamics, and structure and functional studies of proteins using NMR and other spectroscopic techniques.

contributions can be thought of as the "static" and "dynamic" components of ΔG, respectively.[34] Entropy calculations not only must consider the entire protein−ligand complex but also must consider the solvent dynamics.[32,33] The binding of ligand to an enzyme can lead to a decrease (e.g. chorismate mutase[35]), no net change (e.g. α-lytic protease[36]), or an overall increase in protein dynamics (e.g. topoisomerase I[37]) compared to the case of the free enzyme, and this may play an important part in providing ligand affinity. Understanding protein dynamics will lead to a more complete appreciation of its role in ligand recognition and aid in future structure-based drug design programs.[38−40]

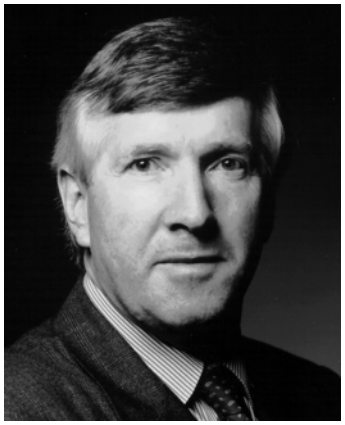

Peter Wright received his B.Sc. degree in Chemistry from the University of Auckland in 1968, his M.Sc. in Chemistry from the University of Auckland in 1969, and his Ph.D. from the University of Auckland in 1972. He received a New Zealand University Grants Committee Postdoctoral Fellowship to the University of Oxford, England, from 1972 to 1976, working under the direction of R. J. P. Williams. Dr. Wright was appointed as a Lecturer in the Department of Inorganic Chemistry at the University of Sydney in 1976, and he was promoted to Senior Lecturer in 1980. He joined the faculty at The Scripps Research Institute as a Professor in 1984 and was appointed in 1987 as the Chairman of the Department of Molecular Biology. He holds the Cecil and Ida Green Chair in Biomedical Research, and he has acted as Editor-in-Chief of *J. Mol. Biol.* since 1990. He received an honorary M.D. degree from the Karolinska Institute, Sweden, in 1995 and an honorary D.Sc. degree from the University of Sydney, Australia, in 2003. His research interests are in applications of NMR to protein folding and intrinsically unstructured proteins, solution structure and dynamics of proteins, and protein–nucleic acid interactions.

1.2. Studying Protein Dynamics

Proteins undergo a wide range of motions in terms of both time and distance scales. There are atomic vibrations on the subpicosecond time scale, pico- to nanosecond backbone and side-chain fluctuations, millisecond conformational rearrangements, and slow breathing modes on the order of seconds[4,41] (Figure 1). Any of these motions may be functionally significant and directly related to ligand exchange and/or catalysis. Motions of backbone and side-chain atoms may be required for molecular recognition, loop motions may be required to exclude water or for repositioning of catalytic residues, and large-scale conformational rearrangements may be required to achieve the active form of the enzyme.[1−4] Thus, time scales can cover from 10^{-15} to >1 s over length scales of 10^{-2} to >10 Å.

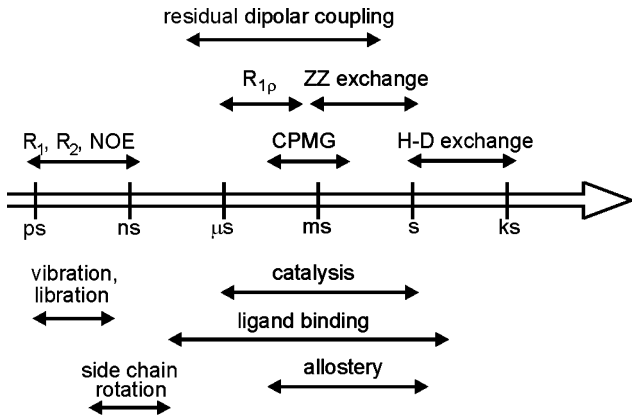

Figure 1. Solution NMR techniques cover the complete range of dynamic events in enzymes.

Many spectroscopic and computational techniques have been developed to monitor various aspects of protein dynamics. X-ray crystallography itself yields some dynamic information. Temperature factors (B factors) are sensitive to the mean square displacements of atoms because of thermal motions and can be obtained for nearly all heavy atoms. However, they do not report on the time scale of thermal motions, and complications related to static disorder, crystal lattice contacts, and refinement protocols make their interpretation difficult.[42] X-ray and neutron scattering also report on protein dynamics. X-ray scattering generally reports on global changes in protein size and shape in a time-resolved manner (reviewed in ref 43), and neutron scattering reports on amplitudes and time scales (10^{-12} to 10^{-8} s) for hydrogen atomic positions in proteins (reviewed in ref 44).

Fluorescence is an important tool in understanding protein dynamics both in the ensemble and in single molecules (reviewed in refs 45−47). Single molecule experiments are proving to be especially informative, leading to an understanding of the motions of individual protein molecules and how this translates into an ensemble signal reported by other methods.[47] Single molecule techniques also offer the exciting possibility of monitoring individual protein dynamics within a true cellular context.

Hydrogen−deuterium exchange mass spectrometry (HX MS) (reviewed in refs 48 and 49) and related techniques, such as radical footprinting (reviewed in ref 50), have been very successful in studying protein dynamics in large supramolecular complexes. With HX MS, not only can dynamic information be obtained for specific sites within individual proteins, but the technique is even more powerful when studying much larger, more complex protein assemblies.[48,49] The motion of the entire complex and individual proteins, and the dynamics of macromolecular assembly can all be studied by time-resolved HX MS (see, e.g., the 30S ribosome assembly in ref 51).

More specialized techniques such as Mössbauer (reviewed in refs 52 and 53), Raman (reviewed in ref 54), and 2D infrared[55,56] spectroscopy are also providing new insights into protein and ligand dynamics. Computer simulations are widely used to study protein dynamics.[57,58] Molecular dynamics has been traditionally limited to very short time scales (femtosecond to nanosecond) in relatively small proteins, but increasing computer power, better theoretical frameworks, and newer methodologies have been increasing both the time scales and the protein sizes amenable to computer simulation.[58,59] Computer simulations serve as a theoretical basis for predicting protein motion, analyzing inputs from the wide variety of experimental techniques, and probing dynamic information beyond what can be assessed experimentally.

NMR, the focus of this review, is an especially powerful experimental technique for studying protein dynamics. The time scale available to NMR techniques ranges over 17 orders of magnitude (10^{-12} to 10^{5} s), covering all of the relevant dynamic motions in proteins. With newer labeling strategies, nearly every atomic site can be probed with NMR-active nuclei.[60] Probes are monitored simultaneously, yielding not only a qualitative picture of protein dynamics but in many cases also a complete kinetic and thermodynamic profile of the dynamic process. Newer TROSY (transverse relaxation optimized spectroscopy) techniques are expanding the traditional size limitations of NMR,[61,62] reaching up to the 900 kDa GroEL complex,[63] with dynamics studies being carried out on the 82 kDa enzyme malate synthase G[64] and the 300 kDa protein ClpP.[65] New in-cell NMR methodology also has the potential to provide complementary information to fluorescence studies in a biological setting.[66,67] NMR provides a complete and thorough description of protein dynamics at a wide range of time scales at atomic resolution without the introduction of bulky, potentially interfering, probes.

While new methodology is being developed to study RNA/DNA enzymes,[68,69] and preliminary data point to the importance of dynamics for these catalysts,[70,71] this review will focus solely on protein dynamics and solution NMR. There have been many reviews concerning NMR methodology applied to protein dynamics[16,21,22,42,72−78] including a recent one that goes into much greater theoretical detail than we do here.[79] The focus of the current review will remain on enzyme dynamics, although similar techniques have been applied to protein folding and protein−protein, protein−DNA, and nonenzyme receptor−ligand interactions.[16,21,42,74]

An important aspect that permeates much of our discussion is the concept of energy landscapes and conformational "substates". Protein folding is generally discussed in terms of an energy landscape "folding funnel" that describes the thermodynamic progression through conformations or "substates" leading to the folded or "ground-state" conformation of the protein.[80−85] Multiple folding paths, consisting of different combinations of substates, are available, and together, all available protein conformations represent the conformation ensemble. The same framework can be applied to folded proteins.[84−87] Multiple protein conformations may exist in thermal equilibrium in solution, in contrast to what may be ascertained from static 3D structures. Structures solved using X-ray crystallography or NMR generally represent the lowest energy conformation and the time-averaged conformational ensemble, respectively. The "ground-state" conformations may comprise >90% of the ensemble, but the sparsely populated, higher energy conformations can also play important roles in the catalytic cycle of an enzyme.

This review will begin with a description of the NMR methodology, followed by a discussion of selected enzyme examples to explain important insights that have been gained into protein dynamics and enzyme function from NMR studies. We conclude with a general discussion relating the "energy landscape" hypothesis to enzyme catalysis.

2. NMR Structural Probes for Protein Dynamics

Even before NMR was used to generate three-dimensional protein structures, one-dimensional ^{13}C relaxation experiments were devised to study protein dynamics.[88−95] The complexity of protein NMR spectra and the low natural abundance of the non-proton NMR-active nuclei ^{13}C and ^{15}N required the development of multipulse, multidimensional NMR experiments and new isotopic enrichment strategies for efficient measurement of protein relaxation.[60,96−107] There have been a few studies that utilize isotopes such as ^{19}F (e.g. 5′-fluorotryptophan in TIM[108]) and ^{31}P (e.g. phosphorylation sites in PKA[109]), but by far, the most common nuclei employed are ^{15}N, ^{13}C, ^{2}H, and ^{1}H to study both backbone and side-chain motions. Uniform or nonspecific labeling with ^{15}N, ^{13}C, or ^{2}H can be readily achieved by overexpressing proteins in *Escherichia coli* grown in minimal medium with a ^{15}N-labeled nitrogen source ($^{15}(NH_4)SO_4$ or $^{15}NH_4Cl$), a ^{13}C-labeled carbon source (e.g. ^{13}C-glucose), or $^{2}H_2O$.[60] More complex labeling schemes are also available for studying

specific side-chain dynamics,[60,106,110−115] and heterologous expression is being explored with other organisms such as the yeast *Pichia pastoris*.[116]

2.1. Picosecond to Nanosecond Time-Scale Motions

2.1.1. Fast Backbone and Side-Chain Motions

Backbone and side-chain fluctuations occur on the picosecond to nanosecond (ps−ns) timescale. These are traditionally studied in NMR by measuring three relaxation rates: the longitudinal relaxation rate, R_1, the transverse relaxation rate, R_2, and the steady-state heteronuclear NOE.[99] Molecular motion in the B_0 field is closely coupled to nuclear spin relaxation; molecular reorientation leads to fluctuating magnetic fields that cause transitions between nuclear spin states and cause coherences to dephase. The spectral density function, $J(\omega)$, is proportional to the amplitude of the fluctuating magnetic field at the frequency ω and is directly related to the three relaxation rates. In the earliest studies of ps−ns time scale protein dynamics, various models for protein internal motion were used to generate different spectral density functions that were then compared to the experimental data. Subsequently, Lipari and Szabo[117,118] generated a spectral density function that is independent from any specific physical model for bond reorientation,

$$J(\omega) = \frac{S^2\tau_m}{1+\omega^2\tau m^2} + \frac{(1-S^2)\tau}{1+\omega^2\tau^2} \quad (1)$$

in the case for isotropic tumbling, where τ_m is the correlation time for the overall rotational diffusion of the macromolecule, S^2 is the order parameter, and $1/\tau = 1/\tau_m + 1/\tau_e$, where τ_e is the time scale (ns) for the internal bond vector (e.g. N−H) motions. An order parameter of 1.0 indicates complete restriction of internal motion, and 0.0 indicates unrestricted isotropic internal motion. It should be noted that it is possible to interpret S^2 in a physical framework.[117,119] The simplest model relates S^2 to "diffusion in a cone" with semiangle, θ,

$$S^2 = \frac{\cos^2\theta(1+\cos\theta)^2}{4} \quad (2)$$

The Lipari−Szabo formalism is also known as "model-free" analysis and is by far the most common interpretation of ps−ns enzyme dynamics; we will limit our discussion to this framework, although we note that alternative approaches such as the SLRS (slowly relaxing local structure) model[120] have proved useful. Newer developments have taken into account anisotropic macromolecular tumbling,[121−125] further parametrization of S^2 into picosecond (S^2_f) and nanosecond (S^2_s) contributions[126] when required by model selection, and application of multiple magnetic field strengths.[124,127−129]

Most studies have focused on N−H bond vectors of the backbone or selected side chain residues, but a similar framework can be used with ^{13}C and ^{2}H to gain a more comprehensive understanding of the fast time scale motions in enzymes (Table 1). In particular, analysis of both $^{15}N-^{1}H$ and $^{13}CO-^{13}C_\alpha$ bond vectors can yield more complete information regarding the ps−ns time scale motions of the protein backbone.[130−132] These vectors point in different directions and can therefore sense different reorientational motions of the peptide plane. Internal motion about an axis parallel to the N−H bond vector would not contribute to the relaxation of the ^{15}N spin but could be sensed by corresponding ^{13}C relaxation experiments.[130−132] Studies on the ribonuclease binase demonstrate that measuring ^{15}N relaxation alone can lead to underestimations of the backbone dynamics and incorrect physical models describing the dynamics.[130]

Fast time-scale motions of the side chains can be readily accessed by studying methyl dynamics in uniformly ^{15}N, ^{13}C and partially ^{2}H labeled proteins (Table 1). ^{2}H relaxation is primarily quadrupolar, making contributions from other processes such as cross-correlation with neighboring $^{1}H-^{13}C$ dipoles or relaxation from other nonbonded spins insignificant, thereby simplifying analysis.[133] The deuterium relaxation is contained within a conventional constant-time ^{1}H, ^{13}C-HSQC experiment, eliminating the large deuterium line widths, and measurements are based on the attenuation of the cross-peaks in a simple 2D $^{1}H-^{13}C$ spectrum.[104] Multiple coherence relaxation pathways can be assessed for ^{2}H, providing high internal consistency.[134,135]

Studies on side-chain dynamics often reveal a richer tapestry of motions than backbone measurements alone. In fact, protein backbone motions remain very poor predictors of side-chain motions.[136,137] While there is a general decrease in the methyl order parameter as the separation from the backbone increases, there is only a very weak correlation between the backbone amide order parameter (S^2_{NH}) and the alanine methyl axis order parameter (S^2_{axis}), and there is no significant correlation for any other amino acid residue.[137] This has been shown to be the case for the enzyme dihydrofolate reductase (DHFR).[138] Order parameters (S^2_{axis} and S^2_{NH}) collected from two complexes, with folate (E:

Table 1. Multiple NMR Probes for Studying Picosecond to Nanosecond Time Scale Motions in Enzymes

relaxing nuclei	bond vector	enzyme example	protein size (kDa)	pulse sequence ref
^{15}N	backbone N−H	staphylococcal nuclease		99
	Trp, N−H			
	Arg, HN−H			*a*
^{13}C	$C_\alpha-CO$			*b*
	$OC-C_\alpha$			*c*
	$C-HD_2$	HIV protease	22	287
	$C-HD_2$	malate synthase G	82	327
^{2}H (D)	backbone D−N			*d*
	methyl D-CH_2	dihydrofolate reductase	18	104
	methyl D-CDH	malate synthase G	82	327
	methylene D-CH			*e*

[a] Pascal, S. M.; Singer, A. U.; Yamazaki, T.; Kay, L. E.; Forman-Kay, J. D. *Biochem. Soc. Trans.* **1995**, *23*, 729. [b] Yamazaki, T.; Muhandiram, R.; Kay, L. E. *J. Am. Chem. Soc.* **1994**, *116*, 8266. [c] Dayie, K. T.; Wagner, G. *J. Am. Chem. Soc.* **1997**, *119*, 7797. [d] Xu, J.; Millet, O.; Kay, L. E.; Skrynnikov, N. R. *J Am. Chem. Soc.* **2005**, *127*, 3220. [e] Yang, D. W.; Mittermaier, A.; Mok, Y. K.; Kay, L. E. *J. Mol. Biol.* **1998**, *276*, 939.

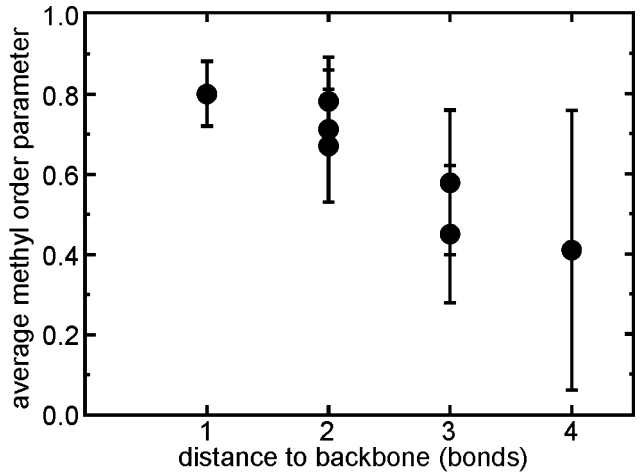

Figure 2. The methyl order parameters (S^2_{axis}) increase as a function of distance from the backbone in *E. coli* dihydrofolate reductase. Data for the figure are taken from ref 138.

folate) and folate plus $NADP^+$ (E:$NADP^+$:folate) bound, demonstrate that the methyl order parameters decrease as the distance from the backbone increases (Figure 2), but there was significant variation for any given methyl type.[138] The variation for S^2_{axis} also decreased with the number of intervening bonds from the backbone.[138]

There have been a few attempts to reconcile dynamic and structural characteristics of proteins. Not surprisingly, amino acids with smaller side chains tend to have greater backbone flexibility.[139] However, the variation of S^2_{NH} is larger than the differences between the averages for different amino acid types. Backbone amide order parameters are also only weakly affected by secondary structure elements, with loops having only slightly smaller average S^2_{NH} values than helices or β-structures.[99] Backbone S^2_{NH} values can be predicted from structures using a simple model that takes account of local contacts to the NH and CO atoms of each peptide group.[140] A more sophisticated model for predicting dynamics from structure has recently been reported. [141] There is also a weak correlation of side chain order parameters with contact distance between the methyl carbon and neighboring atoms and with solvent exposure.[137,142] Finally, a weak correlation between S^2_{axis} and sequence conservation has been observed, suggesting side-chain dynamics may be restricted in some evolutionarily conserved structural motifs.[143] These results demonstrate that dynamics are strongly influenced by the unique three-dimensional architecture of the protein and cannot be readily predicted by the primary sequence or secondary structure of the enzyme. It is an intriguing notion that evolution may have selected for protein dynamics as well as structure, and as will be shown, dynamics affects all stages of enzymatic catalysis.

2.1.2. Order Parameters and Configurational Entropy

Protein folding has been described as a thermodynamic balance between the entropic penalty incurred on going from a highly disordered unfolded state to a highly ordered folded state, and the compensating increase in entropy realized from the release of water molecules that solvate the hydrophobic groups in the unfolded protein.[144,145] The conformational entropy of the unfolded protein may be smaller than previously theorized,[146] and NMR studies [147,148] demonstrate that the folded protein core is not at all rigid. This has implications for the thermodynamic balance sheet for protein folding, which we will not discuss here, but can also have an impact on ligand exchange and catalysis in enzymes.

There have been attempts to reconcile order parameters for the fast-time scale motions with thermodynamic parameters such as entropy and heat capacity,[149−153] but there is still no widely implemented method for quantifying entropy based on fast time-scale motions. Regardless, S^2 can still serve as a qualitative "entropy meter",[16] reporting in a site-specific manner on the loss, gain, and/or redistribution of configurational entropy through different conformational states of an enzyme.

Ligand binding to a protein results in the loss of six rotational degrees of freedom at a potential cost of 20−30 kcal/mol.[14] This can be offset by the presence of six new degrees of freedom and the appearance of new vibrational modes within the complex.[14] Thus, as generally assumed, ligand binding can result in the rigidification of the protein,[33,154−156] but it can also result in an overall increase in protein dynamics or the redistribution of configurational entropy to sites outside the ligand binding pocket (Table 2).

Upon substrate binding, active sites and binding pockets may become more rigid to exclude water or to position important catalytic residues. Loops and flaps commonly close over substrates and/or inhibitors and become more ordered, such as those in β-metallo-lactamase,[157,158] chorismate mutase,[35] HIV protease,[159] dihydrofolate reductase,[160] and hypoxanthine-guanine-xanthine phosphoribosyltransferase (HGPRT).[161] Known catalytic residues often become more ordered on the ps−ns time scale, such as in ketosteroid isomerase[162] and ribonucleaseA (RNase A).[153] The restriction of protein motion within the substrate-bound state may act to limit diffusion from the active site to retain substrate or reactive intermediates, exclude water to maintain a conducive dielectric environment,[163,164] constrain substrate into a conformation resembling the transition state to form a "near-attack-conformation" (NAC),[165] and/or optimally align reacting molecular orbitals via "orbital steering".[166] Regardless of the specific catalytic mechanism, the system must pay a thermodynamic price for ordering the active site. The favorable enthalpy contribution to the enzyme−substrate interaction, or the "intrinsic binding energy",[155] may partially or fully compensate for the entropic penalty. It is also possible that although the active site becomes more ordered upon binding substrate, there is a redistribution of entropy throughout the rest of the system. In ketosteroid isomerase, NMR studies have shown that while Tyr14, the active-site general acid, becomes highly structured upon binding the product analogue 19-nortestosterone hemisuccinate,[167] the majority of residues outside the binding pocket become less ordered (Figure 3).[168] Similar phenomena have been observed in adenylate kinase,[169] oxalocrotonate tautomerase,[170] thiopurine methyltransferase,[171] and topoisomerase I.[37] Redistribution of entropy may occur throughout the protein, as observed in topoisomerase I,[37] or there may be specific distal regions that become less ordered upon ligand binding. For example, in the bound form of adenylate kinase, increased motion is localized to two loops that act as a "substrate binding energy counterweight" (Figure 4).[169,172] In other enzymes, motion increases either at subdomain[37] or intersubunit[168,170] interfaces, raising the intriguing possibility that protein dynamics plays a role in allosteric regulation.[32,173−177]

Table 2. Complex Changes in Enzyme Dynamics upon Binding Ligand

enzyme	ligand	comparison between (f)ree and (b)ound enzymes: S^2	R_{ex}	notes	ref
		Overall Decrease in ps−ns Time Scale Motions upon Ligand Binding			
adenylate kinase	two-substrate mimic AP_5A[a]	b > f	b < f	partial redistribution of ps−ns time scale motions	172
barnase	barstar	b > f	n.a.		*b*
chorismate mutase	transition-state analogue	b > f	b < f	decrease in both ps−ns and μs−ms motions	35
HIV protease	inhibitor DMP323	b > f	b > f	overall decrease in ps−ns motions but new μs−ms motions, especially at the dimer interface	159
malate synthase G	pyruvate and acetyl CoA	b > f		partial redistribution of ps−ns methyl side chain dynamics	327
phosphoribosyl transferase	PRPP[c] and GMP	b > f	n.a.	specific ^{15}N histidine showed reduced ps−ns motion	161
RNase A	inhibitor pTppAp[d]	b > f	b ∼ f		153
RNase H	Mg + AMP	b > f	b > f	ps−ns motions are damped, but new μs−ms motions appear	317
RNaseT1	2′-GMP	b > f	n.a.		*e*
		Overall ps−ns Time Scale Motions Similar between Apoenzyme and Complexed Enzyme			
α-lytic protease	inhibitor peptide boronic acid[f]	b ∼ f	b < f	ps−ns motions remain similar, but exchange processes in binding pocket stabilized	36
hen lysozyme	tri-*N*-acetyl-chitotrioside	b ∼ f	b ∼ f	redistribution of both ps−ns and μs−ms time scale motions	*g*
human lysozyme	tri-*N*-acetyl-chitotrioside	b ∼ f	b > f	redistribution of both ps−ns and μs−ms time scale motions, but increased R_{ex}	*h*
metallo β-lactamase	inhibitor SB225666	b ∼ f	b ∼ f	similar S^2 and R_{ex} terms, but general increase in τ_e, reporting on ns motions	158
4-oxalocrotonate tautomerase	inhibitor *cis*,*cis*-muconate	b ∼ f	b > f	ps−ns motions decrease at intrasubunit interfaces but increase at intersubunit interface, new μs−ms motions appear	*i*
thiopurine methyl-transferase	substrate analogue sinefungin	b ∼ f	b < f	ps−ns motions increase in core but decrease in the less conserved periphery; some μs−ms motions are damped	171
xylanase	trapped glycosyl-enzyme intermediate	b ∼ f	b < f	ps−ns motions similar, but loss of μs−ms motions	*j*
		Overall Increase in ps−ns Time Scale Motions			
3-ketosteroid isomerase	19-nortestosterone hemisuccinate	b < f	b ∼ f	some tightening around binding pocket but increase in motion throughout protein, especially dimer interface	168
topoisomerase I	ssDNA	b < f	b > f	general increase in ps−ns motions, especially in intersubdomain region, also new μs−ms time scale motions	37

[a] $AP_5A = P^1,P^5$-bis(5′-adenosine)pentaphosphate. [b] Sahu, S. C.; Bhuyan, A. K.; Udgaonkar, J. B.; Hosur, R. V. *J. Biomol. NMR* **2000**, *18*, 107. [c] PRPP = α-D-5-phosphoribosyl-1-pyrophosphate. [d] pTppAp = 5′-phosphothymidine(3′,5′)pyrophosphate adenosine 3′-phosphate. [e] Fushman, D.; Weisemann, R.; Thüring, H.; Rüterjans, H. *J. Biomol. NMR* **1994**, *4*, 61. [f] *N-tert*-butyloxycarbonyl-Ala-Pro-boroVal. [g] Mine, S.; Tate, S.; Ueda, T.; Kainosho, M.; Imoto, T. *J. Mol. Biol.* **1999**, *286*, 1547. [h] Mine, S.; Ueda, T.; Hashimoto, Y.; Imoto, T. *Protein Sci.* **2000**, *9*, 1669. [i] Stivers, J. T.; Abeygunawardana, C.; Whitman, C. P.; Mildvan, A. S. *Protein Sci.* **1996**, *5*, 729. [j] Connelly, G. P.; Withers, S. G.; McIntosh, L. P. *Protein Sci.* **2000**, *9*, 512.

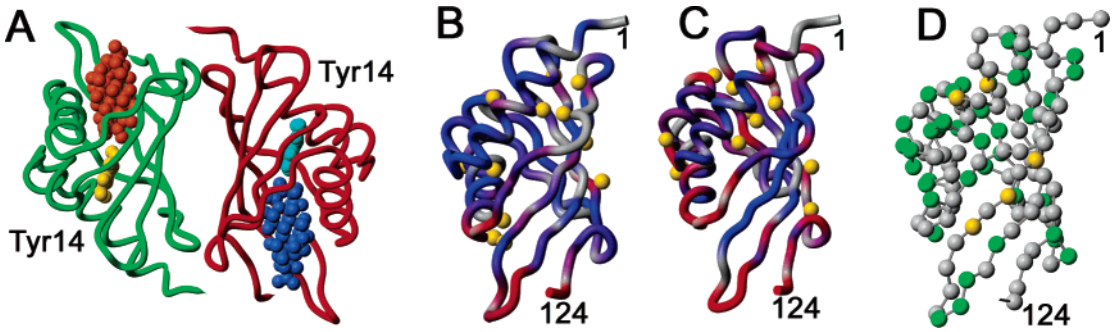

Figure 3. Redistribution of configuration entropy in Δ^5-3-ketosteroid isomerase (KI) upon binding 19-nortestosterone hemisuccinate (cyan). (A) Solution structure (dimer) of KI (PDB 1BUQ) with steroid bound. Monomer units are colored green with orange steroid, and red with blue steroid. The important catalytic residue Tyr 14, which has reduced motion in the presence of ligand, is indicated. (B and C) S^2_{NH} for free and steroid-bound enzyme, respectively, plotted onto the KI backbone using a color scheme ranging from blue ($S^2_{NH} > 0.95$) to red ($S^2_{NH} < 0.8$). Yellow balls indicate residues undergoing conformational exchange ($R_{ex} > 2\ s^{-1}$). (D) Residues with increased ps−ns motion in steroid-bound enzyme (i.e. $S^2_{free} > S^2_{bound}$) are colored green, residues with decreased ps−ns motion in the steroid-bound enzyme (i.e. $S^2_{free} < S^2_{bound}$) are colored yellow, and residues where S^2_{free} and/or S^2_{bound} could not be determined are colored gray. This figure was generated using MOLMOL[354] with data from ref 168.

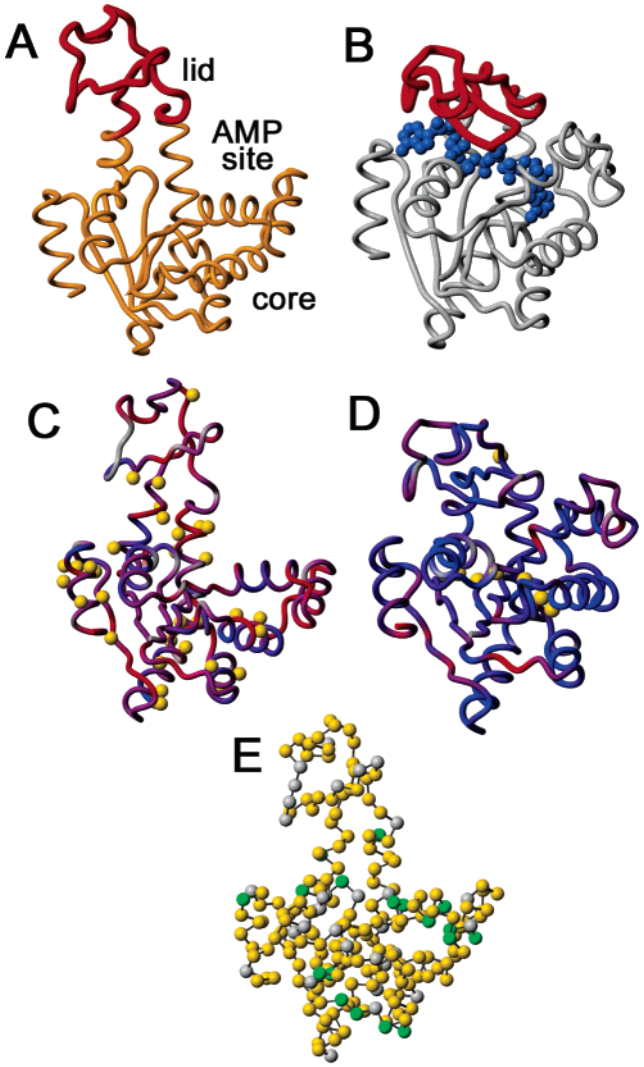

Figure 4. Changes in the backbone dynamics of adenylate kinase upon binding the two-substrate mimic AP_5A. (A and B) Structures of the "open" (PDB 4AKE) and "closed" (PDB 1AKE) AK, respectively, with AP_5A shown in blue and the "lid" domain in red. (C and D) S^2_{NH} for free and AP_5A-bound enzyme, respectively, plotted onto the AK structures using a color scheme ranging from blue ($S^2_{NH} > 0.95$) to red ($S^2_{NH} < 0.8$). Yellow balls indicate residues undergoing conformational exchange ($R_{ex} > 2\ s^{-1}$). (E) Residues with increased ps−ns motion in AP_5A-bound enzyme (i.e. $S^2_{free} > S^2_{bound}$) are colored green, residues with decreased ps−ns motion in the AP_5A-bound enzyme (i.e. $S^2_{free} < S^2_{bound}$) are colored yellow, and residues where S^2_{free} and/or S^2_{bound} could not be determined are colored gray. With AP_5A bound, there are reduced ps−ns and μs−ms motions in AK overall but a small compensatory increase in the ps−ns motions in the "counterweight loops". This figure was generated using MOLMOL[354] with data from ref 169.

2.2. Microsecond to Millisecond Time Scale Motions

2.2.1. Conformational Exchange

R_2 relaxation rates cannot always be fully accounted for in Lipari−Szabo "model-free" analysis in terms of ps−ns time-scale motions, and a new factor, R_{ex}, must be introduced.[73,178] R_{ex} is the relaxation rate due to conformational exchange, as nuclei sample multiple conformations and magnetic environments. This leads to broader cross-peaks that cannot be accounted for by the R_1 and NOE data. Conformational exchange processes generally occur on microsecond to millisecond (μs−ms) time scales and thus report on slower motions than S^2 or τ_e. There is no straightforward relationship between the ps−ns and μs−ms time-scale motions. For example, experiments on enzyme systems have shown that ligand binding that decreases the ps−ns time scale motions may increase, decrease, or not affect the μs−ms time scale motions (Table 2). This obviously also has an effect on the overall entropy contribution, but this has not been fully explored.

Many biological processes occur on the μs−ms time scale, including protein folding, substrate binding, allosteric regulation, and catalysis,[4,22,41] underscoring the importance of studying slower time-scale motions. In a two-site exchange process (A ⇌ B), R_2 measured for substate A depends on the transverse relaxation rate constants in the absence of exchange (R^0_{2A} and R^0_{2B}), the populations of the states (p_A and p_B), the chemical shift difference of the states ($\Delta\omega = |\omega_B - \omega_A|$), and the chemical exchange rate constant k_{ex} ($k_{ex} = k_1 + k_{-1}$) according to the Swift−Connick equation

$$R_2 = p_A R^0_{2A} + p_A p_B K_{ex}\left[\frac{R^0_{2B}(R^0_{2B} + p_A k_{ex}) + \Delta\omega^2}{(R^0_{2B} + p_A k_{ex})^2 + \Delta\omega^2}\right] \quad (3)$$

in the limit of fast exchange ($k_{ex} \gg \Delta\omega$) and when $p_A \gg p_B$.[74,179] More general treatments of the effect of exchange on R_2 relaxation rates are available.[180,181]

Model-free analysis can give only estimates of the magnitude of R_{ex} and thus gives only a qualitative view of μs−ms time scale motions. Failure to correctly account for anisotropic molecular tumbling leads to errors in R_{ex}, further limiting the usefulness of the model-free approach for studying exchange processes. For complete characterization of conformational exchange, $R_1\rho$ or R_2 relaxation dispersion experiments must be used (Table 3). In these experiments, R_{ex} contributions are partially or fully suppressed by applying an external radio frequency (rf) field either by "spin-locking" ($R_1\rho$) or by applying a series of refocusing π pulses in a Carr−Purcell−Meiboom−Gill (CPMG) R_2 relaxation dispersion experiment (Figure 5). Plotting the relaxation rate constant as a function of applied rf field strength then yields dispersion curves that can be fitted to obtain values for k_{ex}, $\Delta\omega$, and $p_A p_B$ (Figure 5). In the case where exchange is fast on the chemical-shift time scale (i.e. $k_{ex} > \Delta\omega$), and assuming $R^0_{2A} = R^0_{2B} = R^0_2$, R_2 is related to the exchange parameters by

$$R_2(1/\tau_{CP}) = R^0_2 + \frac{p_A p_B \Delta\omega^2}{k_{ex}}\left[1 - \frac{2\tanh(k_{ex}\tau_{CP}/2)}{k_{ex}\tau_{CP}}\right] \quad (4)$$

where τ_{CP} is the time between centers of successive π pulses in an R_2 relaxation dispersion experiment and R^0_2 is the transverse relaxation rate constant in the absence of exchange.[79] However, in this regime, only values for k_{ex} and $\Phi_{ex} = p_A p_B \Delta\omega^2$ can be determined.[79] In the slow to intermediate time regime (i.e. $k_{ex} \leq \Delta\omega$), k_{ex}, $p_A p_B$, and $\Delta\omega$ can be deconvoluted by the following equations,

$$R_2(1/\tau_{CP}) = R^0_2 + \frac{1}{2}\left[k_{ex} - \frac{1}{\tau_{CP}}\cosh^{-1}[D_+\cosh(\eta_+) - D_-\cos(\eta_-)]\right] \quad (5)$$

Table 3. Multiple Probes for Studying Conformational Exchange with NMR

probe	group	enzyme example	protein size (kDa)	pulse sequence ref
		R_2 Relaxation Dispersion Experiments		
^{15}N (SQ)	backbone and Trp NH	dihydrofolate reductase	18	*a*
^{15}N (MQ)	backbone and Trp NH			194
^{15}N (ZQ/DQ)	backbone and Trp NH			193
^{15}N (TROSY)	backbone and Trp NH	triosephosphate isomerase	54	196
^{15}N	Asn, Gln NH_2	T4 lysozyme	19	195
^{1}H	backbone and Trp NH	HIV protease	22	199
^{1}H (TROSY)	backbone and Trp NH			193
^{13}C	backbone CO	HIV protease	22	198
^{13}C	backbone C_α			197
^{13}C	side-chain CH_2			
^{13}C	side-chain CH_3	T4 lysozyme	19	208
^{13}C (TROSY)	side-chain CH_3	malate synthase G	82	331
		$R_{1\rho}$ Experiments		
^{15}N	backbone and Trp NH	T4 lysozyme	19	188
^{1}H	backbone and Trp NH			*b*
^{13}C	backbone C_α			*c*

[a] Wang, C.; Grey, M. J.; Palmer, A. G. *J Biomol. NMR* **2001**, *21*, 361. [b] Eichmuller, C.; Skrynnikov, N. R. *J Biomol. NMR* **2005**, *32*, 281. [c] Lundstrom, P.; Akke, M. *ChemBioChem* **2005**, *6*, 1685.

in which

$$D_{\pm} = \frac{1}{2}\left[\pm 1 + \frac{\psi + 2\Delta\omega^2}{(\psi^2 + \zeta^2)^{1/2}}\right]^{1/2} \quad (6)$$

$$\eta_{\pm} = \frac{\tau_{CP}}{2}[\pm\psi + (\psi^2 + \zeta^2)^{1/2}]^{1/2} \quad (7)$$

where $\psi = k_{ex}^2 - \Delta\omega^2$ and $\zeta = -2\Delta\omega(p_A - p_B)$.[79] Data analysis can be made more robust by conducting the dispersion experiments at two or more external B_0 field strengths and fitting residues experiencing the same conformational exchange process with global k_{ex} and $p_A p_B$ values.[182] In favorable cases, the sign of $\Delta\omega$ can also be determined through comparison of HSQC and HMQC spectra at a single spectrometer frequency, or by measurement of HSQC spectra at multiple external field strengths.[180]

By far the most common experiment to study μs−ms protein dynamics utilizes R_2 relaxation dispersion; only a few studies have reported on enzyme dynamics using $R_1\rho$ methodology. However, $R_1\rho$ experiments can use higher effective rf field strengths, allowing the study of faster (μs time scale) motions,[183−187] and there have also been attempts to extend $R_1\rho$ methodology into slower time scales.[188−190] The most common spin probe is ^{15}N, with CPMG pulse sequences available to study single quantum,[191,192] zero quantum,[193] double quantum,[193] and multiple quantum[194] coherences for backbone and side-chain[195] groups in both TROSY[196] and non-TROSY formats (Table 3). The study of multiple coherences is especially relevant when conformational exchange is more complicated than two-site.[193,194] Complementary information can be obtained by studying ^{13}C[197,198] and ^{1}H relaxation dispersion.[198−200] These probes may undergo different conformational exchange processes and give additional insight into the excited protein states being sampled. The chemical shifts of the three nuclei report on different conformational parameters,[201,202] with contributions to ^{1}H and ^{15}N chemical shifts being the most complicated. However, $^{13}C_\alpha$ and ^{13}CO chemical shifts depend primarily on local dihedral angles,[202] potentially enabling direct structural studies on sparsely populated, high energy protein substates. In cases where there is a suitable reference state, $\Delta\omega_N$ and $\Delta\omega_H$ also give valuable structural insight into higher energy conformations,[203] as demonstrated in adenylate kinase (AK),[204] DHFR,[205] and RNaseA.[206] Side-chain μs−ms time-scale motions can also be studied using ^{13}C relaxation dispersion.[207,208]

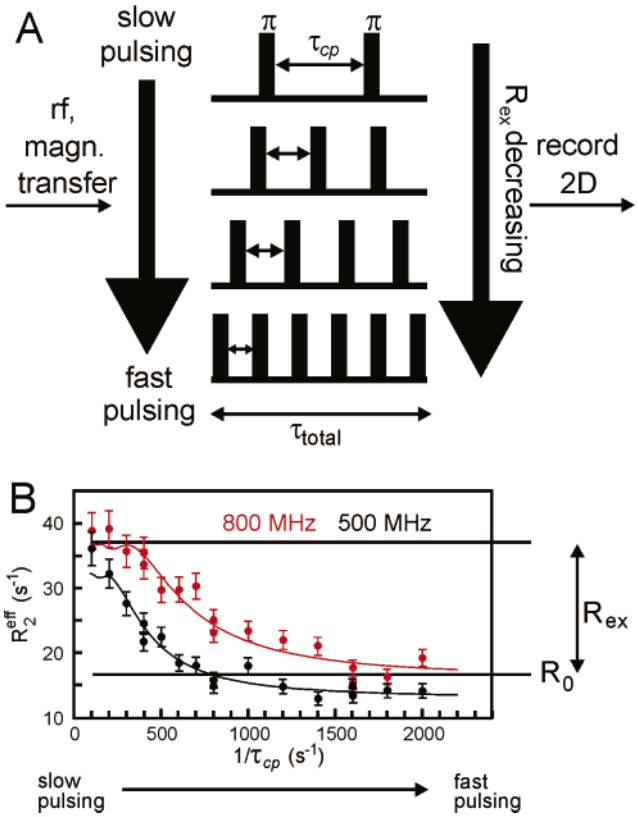

Figure 5. R_2 relaxation dispersion methodology. (A) A series of 2D HSQC spectra are recorded that have different τ_{cp} values. There are generally two π-train segments in a pulse sequence such that the rate constants for the in-phase and anti-phase coherences are averaged.[191] (B) A typical ^{15}N R_2 relaxation dispersion curve. Results are made more robust by conducting the experiment at two or more external magnetic field strengths. For a uniformly ^{15}N-labeled protein, every amide N atom (except for Pro and the N-terminus) potentially yields one dispersion curve, if exchange is on an appropriate time scale, and thus gives site-specific information on the kinetics and thermodynamics of μs−ms time-scale motions.

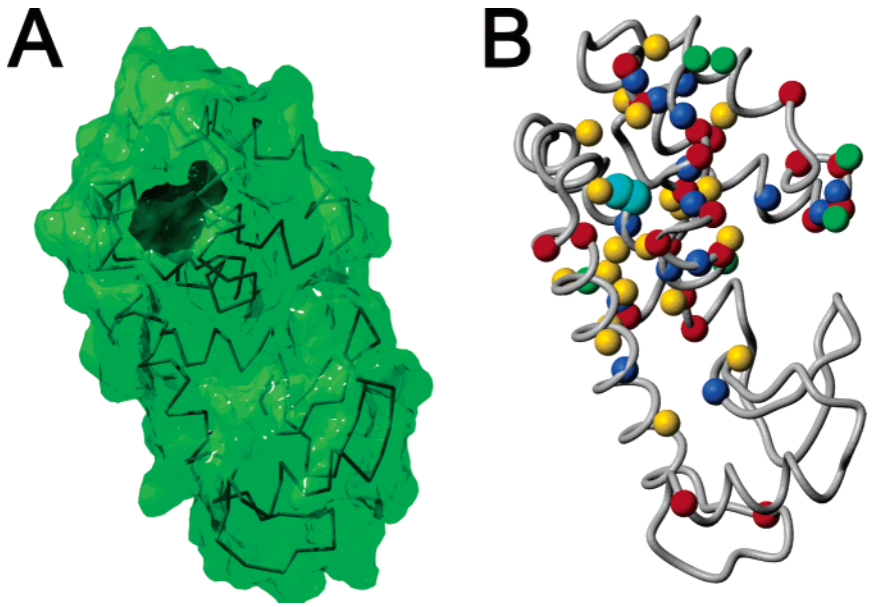

Figure 6. Conformational exchange in T4 lysozyme Leu99Ala (PDB 1L83). (A) Surface representation with the internal cavity generated from mutation of Leu99 to Ala shown in black. (B) Residues with significant R_{ex} using diverse probes, including the ^{15}N backbone (red), ^{15}N Asn/Gln side chains (green), the ^{1}HN backbone (blue), and $^{13}CH_3$ side chains (yellow), are shown with colored balls. Most of the residues showing conformational exchange occur around the pocket created by the mutation (Ala99 in cyan). The enzyme must sample a higher energy conformation that allows access to the internal cavity. This figure was generated using MOLMOL[354] with data taken from refs 195 and 208.

2.2.2. Slow Motions in the Model Enzyme T4 Lysozyme

The power of using R_2 relaxation dispersion experiments in studying μs−ms protein dynamics is exemplified by the enzyme T4 lysozyme. Phage T4 lysozyme has long served as a model system for understanding the relationships between structure, protein folding, and enzyme function.[209−216] More recently, a point mutant of the enzyme, Leu99Ala, has served as a model system for understanding the relationship between ligand binding and μs−ms time-scale motions. This mutation strongly reduces the thermal stability of the protein,[209,210] although the overall three-dimensional structure is nearly identical to that of the wild-type.[217] The most significant change to the structure is the enlargement of an internal cavity that has been shown to bind small, hydrophobic aromatic compounds and xenon,[209−212] even though the cavity is completely buried in the protein interior and is inaccessible to solvent, as judged from the static crystal structure. This suggests that the protein must access a higher energy conformation that somehow exposes the cavity to solvent, thereby allowing entry of xenon and the other ligands.

Model-free analysis showed little change in backbone S^2_{NH} and methyl side-chain S^2_{axis} order parameters between wild-type (WT) T4 lysozyme and the Leu99Ala mutant protein, suggesting similar ps−ns dynamics, but new R_{ex} terms emerged for both backbone and side-chain groups surrounding the cavity in Leu99Ala that were not present in the WT enzyme.[218] This finding prompted further work to study μs−ms time-scale motions using ^{15}N probes for backbone[19] and side-chain[195] groups and ^{13}C probes for methyl side-chain dynamics[19,207] using R_2 and $R_1\rho$[188] relaxation dispersion methods. More than 150 backbone and 75 side chain sites[19] were monitored for conformational exchange. As in the model-free study, only amino acid residues surrounding the cavity showed significant μs−ms time-scale motion[19] in the Leu99Ala mutant that was not present in the WT enzyme[208] (Figure 6). Data for both ^{15}N backbone and ^{13}C methyl side-chain sites were well fit to a two-site exchange model.[19] Individual values for k_{ex} clustered around a narrow distribution and were subsequently fit to a dominant global exchange process with k_{ex} values at 25 °C of 1030 s^{-1} and 1370 s^{-1} for ^{15}N and ^{13}C probes, respectively.[19] The similarity between these exchange rate constants and the off-rate constants of the ligands (325−800 s^{-1}) suggests ligand binding and protein dynamics are coupled.[19] Thermodynamic parameters for the exchange process were also extracted by repeating the experiment at seven temperatures (10−28 °C).[19] The less populated conformation was found to be 2 kcal/mol higher in energy than the ground-state complex, with unfavorable enthalpy (7.1 kcal/mol) and favorable entropy contributions (5.1 kcal/mol). The partially compensating increase in disorder suggested a local unfolding of the protein to allow the ligands access to the internal cavity.[19]

These elegant studies on T4 lysozyme allowed for a complete structural, kinetic, and thermodynamic characterization of the μs−ms time-scale motions for both the backbone and side-chain groups. Similarly, rigorous studies on other enzymes have the capacity to reveal the role that higher energy protein substates play in other aspects of enzyme catalysis. The following case studies will highlight the role of protein dynamics in various phases of the catalytic cycle with special emphasis on the role of μs−ms time-scale motions that are on the same time scale as the events in catalysis.

3. Case Studies in Enzyme Dynamics

3.1. Conformational Selection in Ribonuclease A

RNase A is a small (13.7 kDa) enzyme responsible for cleaving single-stranded RNA, specifically on the 3′-side of pyrimidine residues.[219] The enzyme is secreted from the pancreas and is believed to function primarily as a digestive enzyme.[153,219] RNaseA has a long history in serving as a model enzyme for functional and structural studies (reviewed

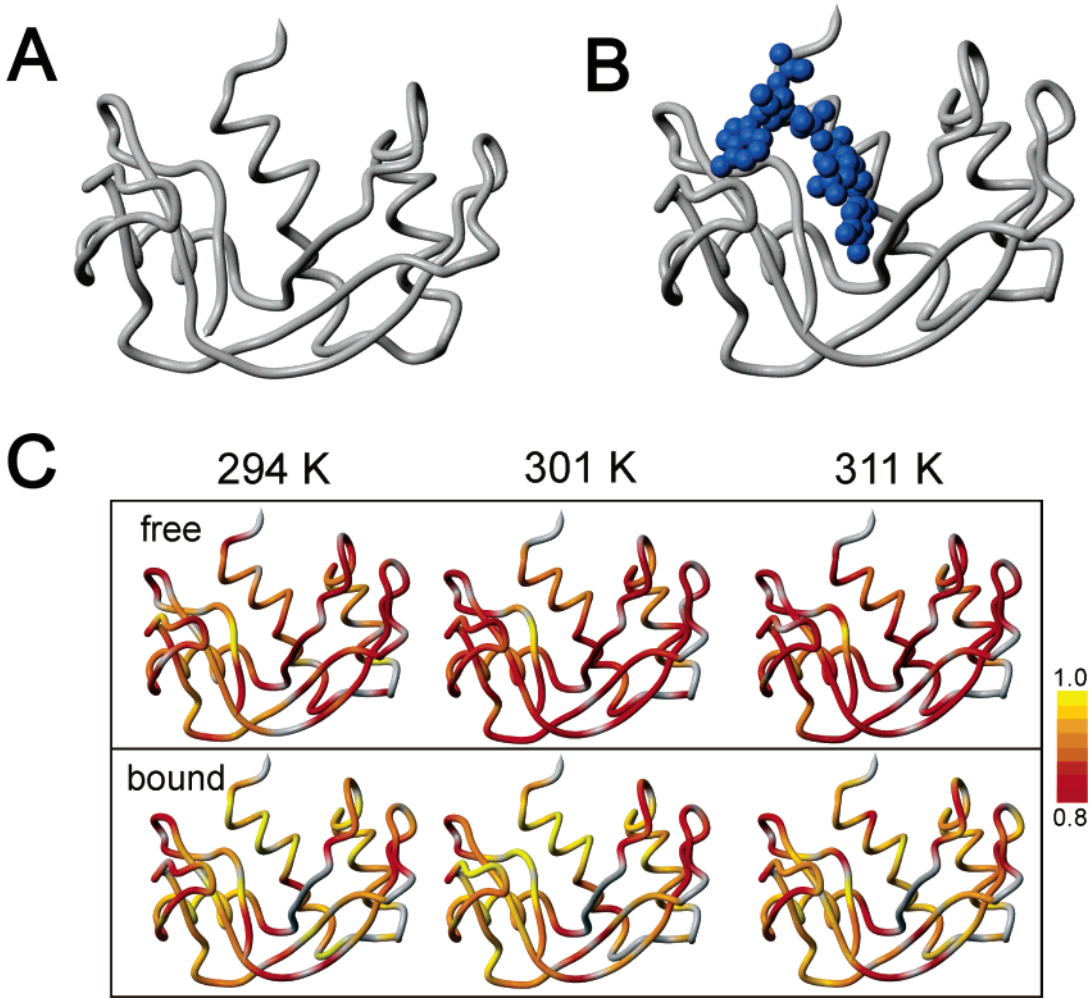

Figure 7. Changes in configurational entropy in ribonuclease A as a function of temperature and ligand binding. (A and B) Structures of RNaseA in the free (PDB 7RSA) and with pTppAp (in blue) bound (PDB 1U1B). (C) Changes in S^2_{NH} with increasing temperature in free (top row) and pTppAP bound (bottom row) enzyme. Panel C is redrawn with permission from ref 153. Copyright 2003 American Chemical Society.

in ref 219). There are over 100 structures of RNaseA in the protein databank (PDB). The enzyme consists of two antiparallel β-sheets, each containing three β-strands, which form a V-shaped motif. Three α-helices and six loop/turn regions pack against the central β-sheet core. The enzyme is further stabilized by disulfide bonds between eight cysteine residues to form a very rigid structure (Figure 7).

Model-free analysis of free RNaseA [153,220] provides direct evidence that the protein is very rigid on the ps−ns time scale. The binding of the nanomolar inhibitor pTppAp (5′-phosphothymidine(3′,5′)pyrophosphate adenosine 3′-phosphate) further increases S^2_{NH} throughout the enzyme (Figure 7).[153] In this case, there is no redistribution of configurational entropy as observed for enzymes such as 4-oxalocrotonate tautomerase,[170] and even residues outside the active-site pocket exhibit increased S^2_{NH} (Figure 7).[153] However, the temperature dependence of S^2_{NH}, a measure of entropy, reveals a redistribution of heat capacity (ΔC_p) upon inhibitor binding.[153] There is no net change in heat capacity but only residue-specific changes with a balance of positive and negative contributions (Figure 7).[153] The NMR measurements are consistent with theoretical calculations[153,221,222] that suggest the backbone provides 40−45% of the residual configurational entropy upon protein folding.

While RNase is rigid on the ps−ns time scale, it is significantly more flexible on the μs−ms time scale. The μs−ms time scale motions are very similar between free and inhibitor bound enzyme (Figure 8).[153,206] ^{15}N R_2 relaxation dispersion allowed for kinetic (k_{ex}), thermodynamic ($p_A p_B$), and structural ($\Delta\omega$) characterization of the conformational exchange processes.[206] A correlation was observed between the $\Delta\omega$ values for the free- and inhibitor-bound enzyme, suggesting that a structurally similar process occurs in both cases (Figure 8).[206] The μs−ms time scale motions in the inhibitor-bound enzyme are not due to ligand binding/release, since the population of free enzyme is only 0.02%, considerably less than the measured population (p_b) of the higher energy conformer.[206] These results suggest that RNaseA is in dynamic equilibrium between two conformations representing the free and inhibitor-bound forms of the enzyme.[206] The agreement between k_{ex} and ligand off-rates observed in RNaseA is consistent with a functional role for the higher energy conformation.[206] In this scenario, the higher-energy protein conformation is responsible for binding ligand in the free form, and the higher-energy conformation in the inhibitor-bound form is involved in the release of ligand. This represents a process of "conformational selection": [83,223−229] a ligand binds to a sparsely populated, higher energy conformation that is more complimentary to the ligand than is the "ground-state" conformation and, through binding, the free energy of the complex is reduced such that the higher energy substate becomes the new highly populated "ground-

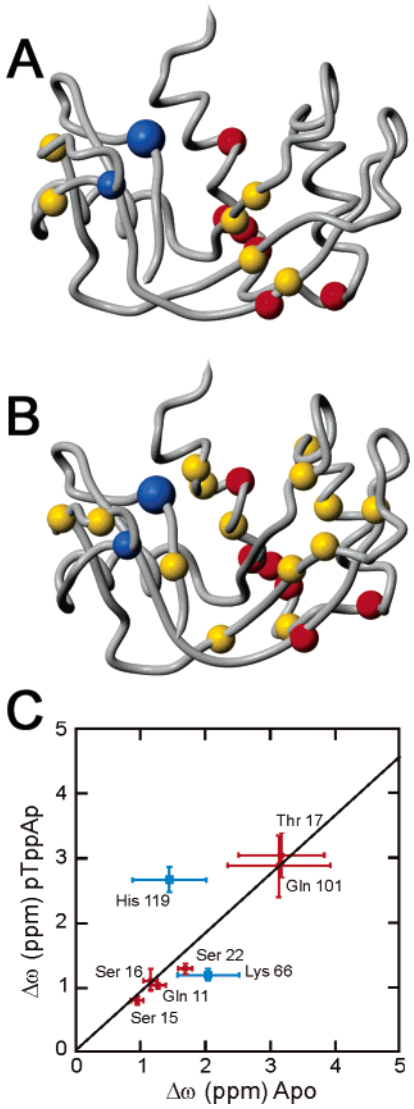

Figure 8. Conformational selection in ribonuclease A. (A and B) Residues with significant R_{ex} from ^{15}N R_2 relaxation dispersion experiments for free and pTppAp-bound enzyme, respectively, are shown as balls. His119 is an important catalytic residue (shown as an enlarged ball). Blue and red balls are color-coded according to the points in panel C, and residues with yellow balls indicate dispersion can only be evaluated for either free or inhibitor bound enzyme. (C) The dynamic chemical shift changes ($\Delta\omega$) between lowest energy and higher energy conformations of RNaseA are similar between free and inhibitor-bound enzyme. Panels A and B were generated using MOLMOL.[354] Panel C is reprinted with permission from ref 206. Copyright 2005 American Chemical Society.

state" conformation (Figure 9). A very recent study shows that a similar process occurs in the 3′-CMP-bound RNaseA product complex.[230] The dynamic process is disrupted by mutating Asp121, a strictly conserved residue that does not make any direct contact with substrate or product.[230] Mutation of Asp121 to Ala results in a 90% loss of catalytic activity.[231] In Asp121Ala, there is "dynamic uncoupling" such that some residues can no longer be fit globally to the same k_{ex}.[230] However, the $\Delta\omega$ values do not change, implying that the structural changes are identical between the wild-type and Asp121Ala.[230] Asp121 is thus conserved not because it is involved directly in the chemical transformation but because it is involved in coordinating dynamic events important for catalysis.[230]

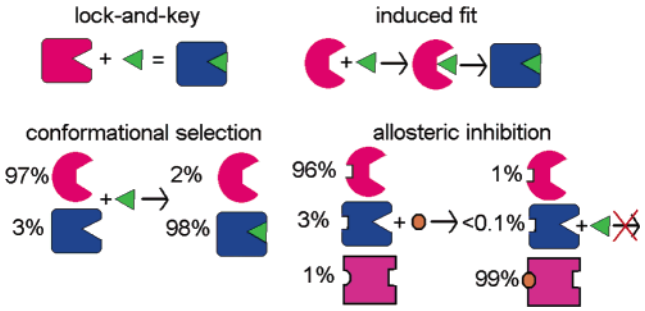

Figure 9. Schematic figure showing potential mechanisms for interaction between enzymes and ligands. Lock-and-key[355] and induced-fit[343] assume conformational homogeneity, but conformational selection[224] takes into account conformational heterogeneity. The conformational ensemble may also be altered by allosteric ligands binding to alternative sites on the enzyme.

Conformational selection is in the spirit of the Monod−Wyman−Changeux (MWC) mechanism of allosteric transitions,[232] and it can now be applied to "nonallosteric" proteins.[83,174,175,228] Enzyme inhibitors disturbing the equilibrium between free and bound conformations would have the ability to reduce substrate binding even if the inhibitor-binding pocket is distant to the active site.[83,175,228] As we will discuss below, NMR and computer simulations suggest that protein dynamics are often correlated between distant, solvent-exposed residues and catalytically important, active-site residues, and thus, an opportunity exists to develop "allosteric" inhibitors for "nonallosteric" enzymes.[233−235] This approach would be especially powerful in situations where inhibitor/drug resistance develops, as it provides additional sites outside the substrate binding pocket that could be targeted. Protein dynamics, revealed by NMR and other techniques, thus provide new complexities and new opportunities in structure-based drug design.[31,38−40]

3.2. Reaction Coordinate Compression in *E. coli* Dihydrofolate Reductase

DHFR is an extremely well characterized enzyme in both structural and mechanistic terms.[5] The enzyme catalyzes stereospecific hydride transfer from C4 of NADPH to the C6 position of 7,8-dihydrofolate (DHF) to form 5,6,7,8-tetrahydrofolate (THF). The enzyme is ubiquitous, and its central role in the maintenance of cellular pools of THF makes it an attractive target for antibacterial, antimalarial, and anticancer agents.[236−238] The complete kinetic mechanism for wild-type *E. coli* DHFR[239] and a number of mutant enzymes has been elucidated.[240−243] The *E. coli* enzyme cycles through five intermediates, E:NADPH, E:DHF:NADPH, E:THF:$NADP^+$, E:THF, and E:THF:NADPH. Importantly, there is rebinding of NADPH prior to the release of THF product so that free enzyme is never generated under steady-state turnover conditions at cellular concentrations of substrate and cofactor. Moreover, the rate-determining step in the catalytic cycle is not hydride transfer but the release of THF from the E:THF:NADPH ternary product release complex.[239]

There are over 40 X-ray structures of *E. coli* DHFR,[5] and importantly, there are isomorphous crystal structures for all of the intermediates or models of the intermediates that delineate the conformational changes that occur throughout the catalytic cycle.[244,245] The 159-residue enzyme consists of a central eight-stranded β-sheet (β-strands A−H) and four flanking α-helices (α_B, α_C, α_E, and α_F) (Figure 10). The

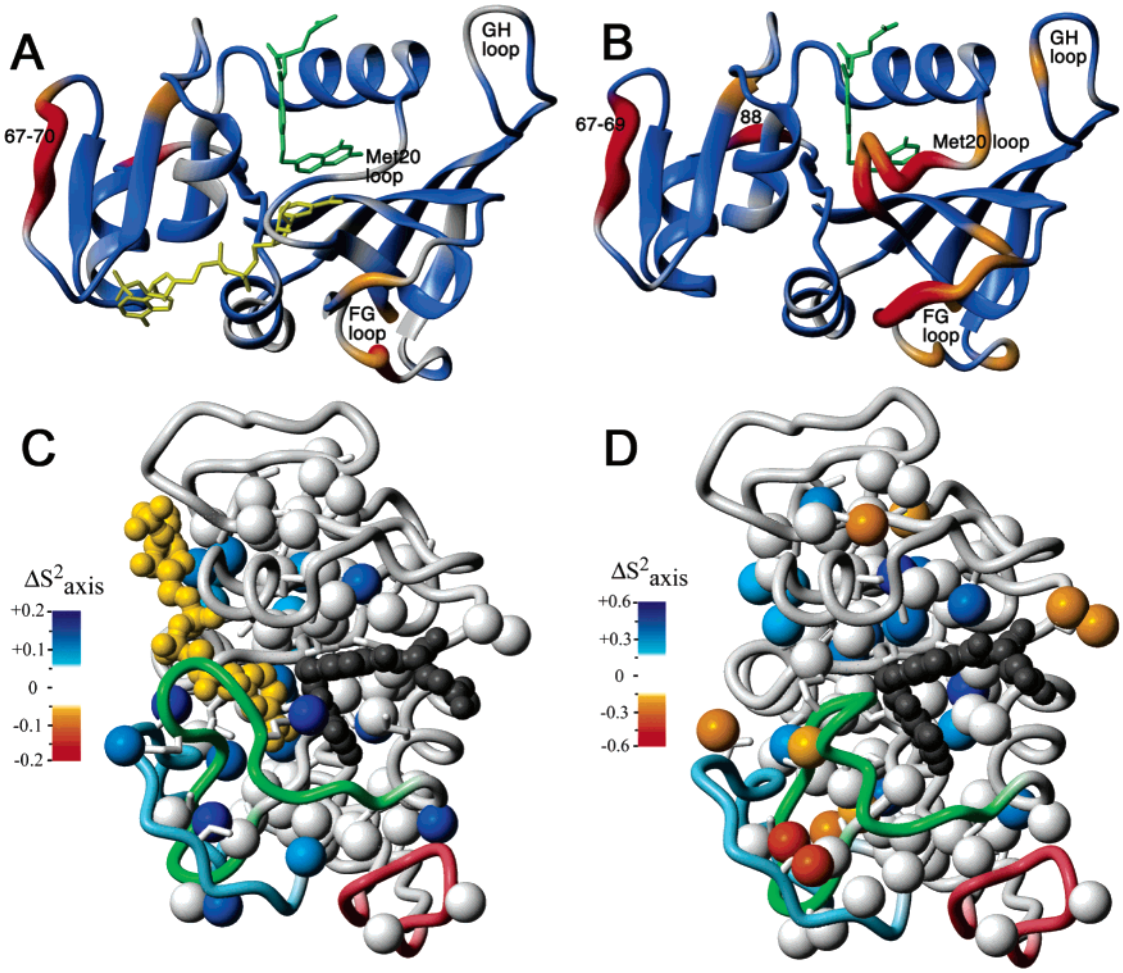

Figure 10. ps−ns time scale motions in dihydrofolate reductase. (A and B) S^2_{NH} plotted onto the structures for E:NADP$^+$:folate (PDB 1RX2) and E:folate (PDB 1RX7), respectively, on a scale from red (with thickened tube) to blue indicating lower and higher values of S^2, respectively. Folate is shown in green, and NADP$^+$ is shown in yellow. (C) Difference in methyl S^2_{axis} between E:NADP$^+$:folate and E:folate. (D) Normalized methyl S^2_{axis} for E:folate. In panels C and D, the Met20 loop is shown in green, the F−G loop in blue, and the G−H loop in pink. Methyl groups are shown as balls, colored according to the scales indicated. Folate is shown in gray, and NADP$^+$ is shown in yellow. Reprinted with permission from refs 138 and 160. Copyright 2004 and 2001 American Chemical Society.

protein can be divided into two subdomains, the smaller adenosine binding domain (residues 38−88) and the major subdomain (sometimes called the loop subdomain), with the active-site cleft between them. The major subdomain contains three important loops: the Met20 loop (residues 9−24) closes over the active-site pocket, and the FG (residues 116−132) and GH (residues 142−150) loops stabilize the various conformations of the Met20 loop. There are four conformations of the Met20 loop that have been observed in the crystalline state, with the *closed* and *occluded* conformations being most important to the catalytic process.[246] In the substrate binding complexes, E:NADPH and E:folate:NADPH, the Met20 loop forms a *closed* conformation; however, upon hydride transfer, there is a *closed*-to-*occluded* conformational change in the Met20 loop[245,246] (Figure 10). In the *occluded* conformation, the nicotinamide ring is pushed out into the solvent and is sterically hindered from entering the active-site pocket. Thus, only the *closed* conformation is conducive to catalysis. The *closed* conformation is stabilized by hydrogen bonds between Gly15 (CO) and Gly17 (NH) of the Met20 loop and Asp122 (NH and Oδ) in the FG loop, but in the *occluded* conformation, these hydrogen bonds are broken and new ones are formed between Asn23 (CO and NH) and Ser148 (NH and Oγ) in the GH loop.[245]

The ps−ns time-scale motions of the enzyme have been probed in three complexes, E:folate, E:folate:NADP$^+$, and E:folate:5,6-dihydroNADPH (DHNADPH).[138,160,247,248] E:folate and E:folate:DHNADPH are both *occluded* complexes and serve as models for the E:THF and product ternary complexes (E:THF:NADP$^+$/E:THF:NADPH), respectively. The Met20 loop in E:folate:NADP$^+$ is in a *closed* conformation with both the pterin ring of folate and the nicotinamide ring of the cofactor inserted into the active-site pocket, and so this complex serves as a model for the E:DHF:NADPH Michaelis complex. Model-free analysis of ^{15}N relaxation data for the two *occluded* complexes gave very similar results.[160] Several residues in the Met20 and FG loops have below-average S^2_{NH} values with internal correlation times on the order of 1−2 ns. However, the motions in the Met20 and FG loops are attenuated in the *closed* Michaelis model complex, with increased S^2_{NH} and/or loss of nanosecond (τ_e) time-scale motion (Figure 10). A similar phenomenon is observed in the side-chain S^2_{axis} methyl order parameters.[138] There is general restriction of the ps−ns time scale motions in the Met20 and FG loops in the *closed* E:folate:NADP$^+$ complex, as compared to E:folate. Side-chain order parameters also increase for those residues around the nicotinamide binding pocket[138] (Figure 10). The tightening of the Met20 loop over the active-site pocket and the decrease in fast time-

scale motions may be important for limiting diffusion into and out of the pocket and for maintaining the nicotinamide ring in a conformation conducive to hydride transfer.

The ps−ns dynamics for the *occluded* complexes E:folate and E:folate:DHNADPH are very similar, suggesting that the determining factor is the *closed* or *occluded* conformation of the enzyme. While the fast time-scale dynamics appear to be ligand nonspecific, R_2 relaxation dispersion studies of the various intermediates in the DHFR catalytic cycle suggest that motions on the μs−ms time scale are influenced by the nature of the bound ligands[205] (Boehr et al., in preparation). Studies of the slower time-scale motions of the *closed* E:folate:NADP$^+$ complex, a model for the Michaelis complex, reveal significant exchange contributions to relaxation at several sites in the polypeptide chain.[205] Chemical shift perturbation studies have identified sets of marker resonances that report on cofactor binding, substrate/product binding, and the *closed*−*occluded* conformational change.[249] The most significant R_{ex} terms for the E:folate:NADP$^+$ complex arise for the "*closed*−*occluded transition*" markers (Figure 11A). Moreover, the $\Delta\omega$ values determined from global fits of the dispersion curves for these and other residues with significant R_{ex} values correlate with the equilibrium chemical shift differences $\Delta\delta$ between the *closed* E:folate:NADP$^+$ complex and the *occluded* E:folate:DHNADPH complex (Figure 11B). This suggests that the E:folate:NADP$^+$ complex, which adopts a *closed* conformation in its ground state, samples a higher energy excited state in which the active-site loops are in the *occluded* conformation. The kinetics for this conformational exchange is very similar to the hydride transfer rate, pointing toward its importance to the catalytic cycle.

The R_{ex} values for the E:folate:NADP$^+$ complex are quite different from those of the E:folate binary complex, determined from model-free analysis[160] and R_2 relaxation dispersion data (McElheny et al., unpublished). In E:folate, R_{ex} terms, which are absent for E:folate:NADP$^+$, are observed for residues whose chemical shifts report on cofactor binding, suggesting that motions in the cofactor binding pocket are important for binding NADP(H). Indeed, the $\Delta\omega$ values for these residues correlate with equilibrium $\Delta\delta$ values for binding of cofactor (unpublished data), suggesting that the enzyme samples a high energy state in which the conformation of the (empty) adenosine binding site resembles that of the cofactor bound complex. These results provide strong support for a mechanism in which cofactor binding occurs by a process of conformational selection.

Slower time-scale motions may also play a critical role in catalysis. Several isoleucine, threonine, and valine residues undergo dynamic rotamer averaging about the χ1 dihedral angle on the μs−ms time-scale, as evidenced by line-broadening.[138] This includes Ile14 and Ile94, which both populate the *gauche*+ and *trans* rotamers in solution; however, in the X-ray structures, only the *gauche*+ conformation is observed.[245] In the *trans* conformation, the side chains of these residues would overlap significantly with atoms of the nicotinamide and pterin rings, respectively. This unfavorable interaction could be overcome by motion of the rings toward one another, thus shortening the hydride donor−acceptor distance (Figure 12). Based on kinetic isotope effects (KIE), the DHFR reaction is significantly influenced by hydrogen tunneling events.[250−253] Hydrogen tunneling and hydride transfer are highly distance-dependent,[254−256] and so, rotamer averaging and side-chain motion could significantly affect enzyme catalysis.[138] Optimal geometry for hydride

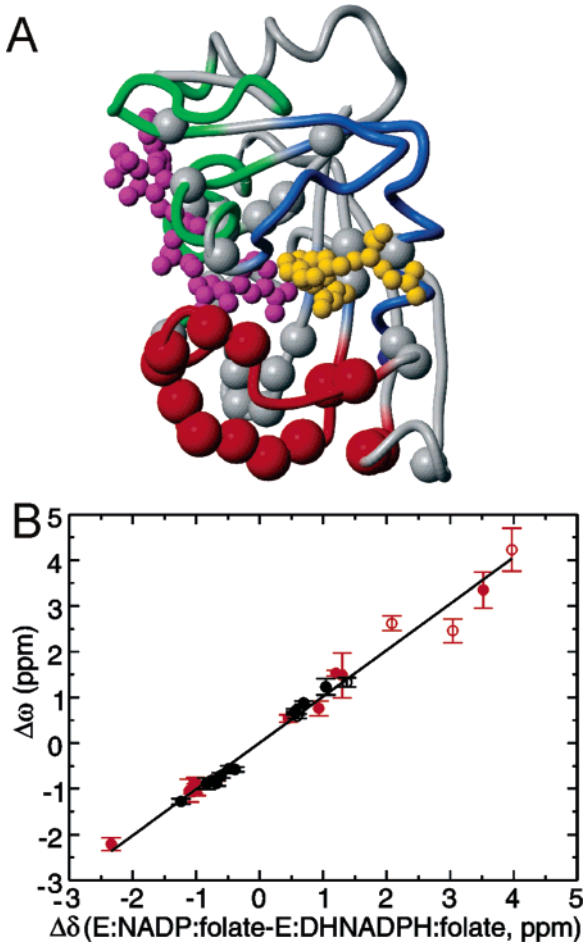

Figure 11. μs−ms time-scale motions in the E:NADP$^+$:folate DHFR complex at 303 K. (A) Chemical shift perturbation studies[249] identified "cofactor-binding" (green), "folate-binding" (blue), and "closed-occluded transition" (red) marker residues. Gray regions indicate residues that do not fall into any of the three marker groups. Residues that exhibit significant exchange contributions in ^{15}N R_2 relaxation dispersion experiments are shown as balls, with red balls indicating the "closed−occluded transition" marker residues.[205] Folate is shown in yellow, and NADP$^+$ is shown in magenta. (B) The correlation between dynamic chemical shift ($\Delta\omega$) and equilibrium chemical shift ($\Delta\delta$) changes indicates that E:DHNADPH:folate, an occluded complex, is a good model for the higher energy conformation of E:NADP$^+$:folate, a closed complex. "Closed−occluded transition" markers are highlighted in red. The sign of $\Delta\omega$ was determined through comparison of HSQC/HMQC spectra[180] for most of the resonances (filled circles).

transfer requires that hydride donor and acceptor atoms approach within 0.8 Å of their van der Waals radii, and thus, the *trans* rotameric substate observed by NMR could play a role in stabilization of the transition state.[255] Consistent with this notion, mutation of Ile14 leads to a 20-fold reduction in the hydride transfer rate.[257] The coupling of motion and hydride transfer has been studied extensively in alcohol dehydrogenases and related enzymes.[258]

Several residues showing rotamer averaging in the E:folate:NADP$^+$ model of the Michaelis complex have similar rotamer distributions (major rotamer $\sim$ 65% and minor rotamer $\sim$ 35%). These include residues Val10, Val13, Ile14, Thr113, Ile115, and Val119,[138] all of which are near each other in the 3D structure (Figure 12), providing strong evidence that the rotamer jumps of these side chains are correlated. This is in marked contrast to the case of the E:folate complex, where rotamer populations are more

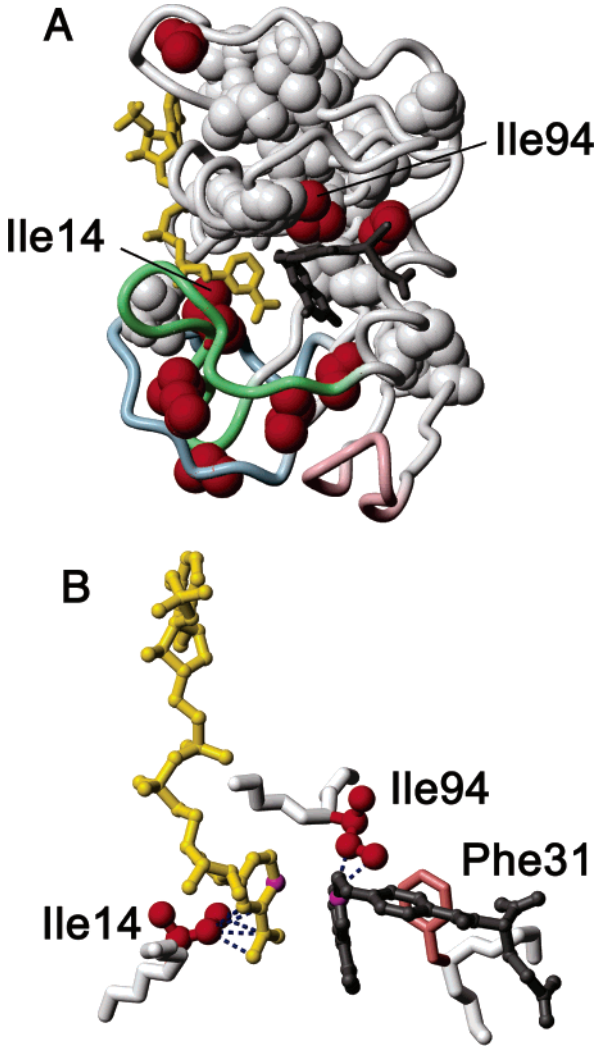

Figure 12. Reaction coordinate compression in DHFR. (A) Residues exhibiting χ^1 rotamer averaging are shown in red, and those residues that exhibit a single rotamer (>70% occupancy) are shown in white. (B) In the minor *trans* rotamer, Ile14 and Ile94 would sterically clash with nicotinamide cofactor (yellow) and folate substrate (dark gray), respectively. Steric clash would be relieved by pushing the pterin and nicotinamide rings toward each other, thus shortening the distance between the hydride donor and acceptor (shown as magenta balls). Reprinted with permission from ref 138. Copyright 2004 American Chemical Society.

heterogeneous.[138] These results are of considerable significance in light of molecular dynamics simulations that demonstrate correlated fluctuations throughout the protein,[259] which may be interpreted in terms of concerted transitions between substates[260−262] or stepwise dynamic coupling.[263−266] In particular, it has been suggested that Ile14 participates in a network of "coupled promoting motions" that facilitate hydride transfer.[265] Coupled motions disappear in other complexes of the enzyme, such as E:THF:$NADP^+$ and E:THF:NADPH,[259] consistent with the observations from NMR experiments on the E:folate complex. Thus, NMR is consistent with computer simulation and KIEs that suggest protein dynamics are intimately linked with hydride transfer.

3.3. Substrate Binding and Drug Resistance in HIV Protease

The human immunodeficiency virus (HIV) protease is an important target for development of drugs against AIDS. The protease is a major determinant in the life cycle of HIV, cleaving the Gag and Pol polyproteins into mature structural proteins, and inhibition of the enzyme leads to the production of noninfectious particles.[267,268] HIV protease has served as a paradigm for structure-based drug design, with several potent protease inhibitors already in clinical use.[269−271] However, the emergence of protease variants resistant to the inhibitors compromises drug treatment.[269−271] While several of the responsible mutations occur around the active-site pocket, distant mutations can also lead to a decrease in inhibitor sensitivity or compensate for activity lost by mutation to the active-site residues.[272] The HIV protease is very plastic and remains a resilient drug target.

The HIV protease is a 22 kDa homodimer. The "flaps" (residues 34−59), a pair of two-stranded β-sheets at the top of the protein, control access to the active-site pocket (Figure 13). Molecular dynamics simulations have also identified the "fulcrum" (residues 11−21) and the "cantilever" (residues 64−74) as regions of increased mobility (Figure 12).[273−276] Crystal structures reveal heterogeneous flap structures, ranging from a closed conformation when inhibitor is bound[277,278] to semiopen conformations.[279−281] However, neither of these conformations allow substrate access to the active site,[277] suggesting that the protein must access minor, higher energy conformations that would allow ligand exchange to occur.

The faster time-scale motions have been compared for free enzyme[159] and enzyme bound to the inhibitors DMP323,[282,283] KNI-272,[284] and P9941.[282] The inhibitor-bound forms display very similar backbone motions on the ps−ns time scale. Smaller than average S^2_{NH} values are observed for residues 17−19 in the fulcrum, 38−42 in the flaps, and 69−71 in the cantilever,[282,284] in agreement with molecular dynamics simulations[274] (Figure 13). The smallest S^2_{NH} values are found for residues in the loops of the flaps, sometimes called the "flap elbows". The free enzyme has similar regions of increased flexibility, and in addition, the flap "tips" (residues 49−53) have below average S^2_{NH} values[159] (Figure 13).

The increased ps−ns time-scale motions in the flap tips of the free HIV protease have led to the suggestion that these motions may be important for further opening of the flaps to allow ligand access to the active site.[159] Experiments that probe motions at slower time scales also indicate that the flap tips are flexible on the μs−ms time scale,[285] for both free and inhibitor-bound enzymes (Figure 13). R_2 relaxation dispersion experiments have been used to probe the backbone dynamics of the DMP323-bound enzyme using ^{1}H amide,[198−200] ^{15}N,[198−200,285] and ^{13}CO[198] relaxation experiments. The use of multiple probes allows for a more complete dynamic picture.[198] Depending on chemical shift differences between the lowest energy and higher energy protein conformations, different R_{ex} values are observed for the various nuclei. The different probes thus supply complementary data and give more detailed structural insights into the higher energy conformations (Figure 13).[198]

In addition to the residues in flap tips, residues in the intersubunit β-strand also undergo significant conformational exchange processes reflected by both main-chain[198−200,285] and side-chain resonances.[286,287] The μs−ms motion is increased upon binding inhibitor,[285] suggesting redistribution of entropy onto a longer time scale. The increased motion at the dimer interface may be biologically relevant and may play a role in the maturation process of the protease.[285]

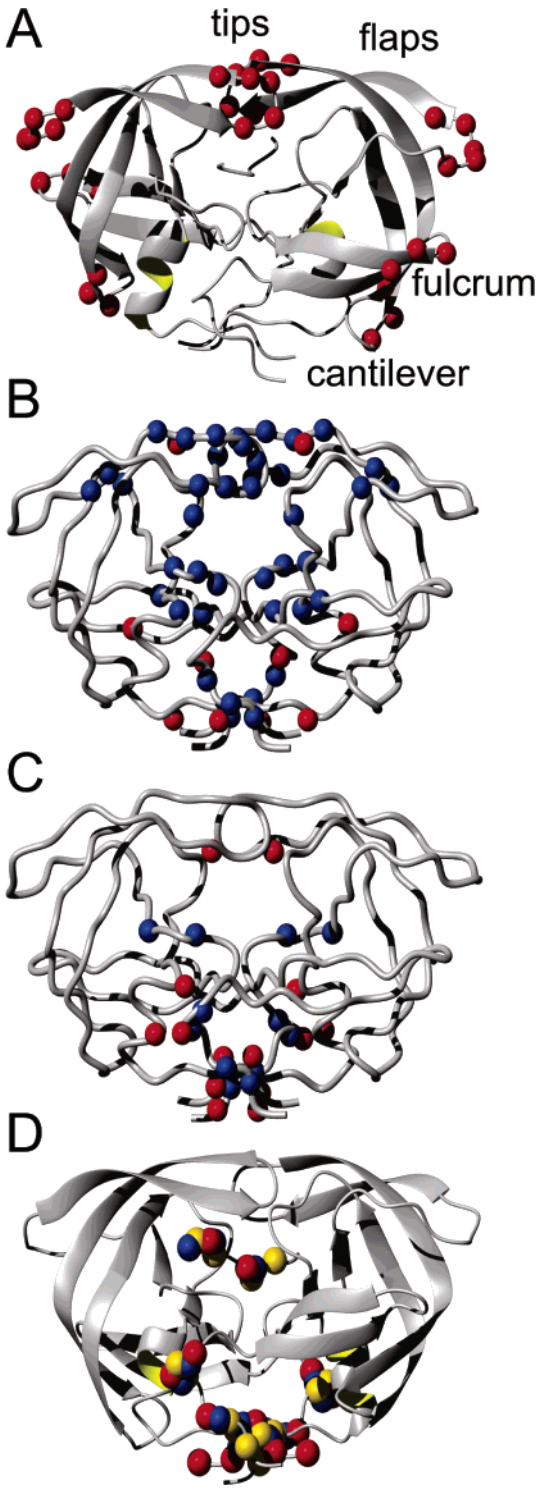

Figure 13. Multiple time-scale motions in the free and inhibitor bound HIV protease. (A) The HIV protease homodimer bound with DMP323 (PDB 4PHV) shows decreased S^2_{NH} primarily in three regions: the flap "elbows", the fulcrum, and the cantilever. Free enzyme also shows decreased S^2_{NH} in the flap tips. (B and C) μs−ms motion in free and DMP323 enzyme, respectively, with residues showing significant R_{ex} from ^{1}HN (blue) or ^{15}N (red) relaxation studies shown as colored balls. (D) R_2 relaxation dispersion studies with ^{1}HN (blue), ^{15}N (red), and ^{13}CO (gold) identify other residues undergoing conformational exchange, indicated by colored balls. The dimer interface is especially dynamic on the μs−ms time scale that may be important for function, and identifies this region as a potential target for inhibitor design. This figure was produced using MOLMOL[354] with data from refs 159, 198, and 285.

Regions with reduced S^2 values, including the flaps, fulcrum, and cantilever, may be related in their dynamical processes, but NMR alone is not able to decipher these interactions. Molecular dynamics simulations can recapitulate the experimental S^2_{NH} values, and computer simulations further suggest that the ps−ns protein motions are correlated.[273] The coupling of the motions between the flaps, fulcrum, and cantilever is also correlated to motions of the substrate that are important for catalysis.[273] This is analogous to the situation observed in DHFR, but here, promoting motions are important for heavy atom, rather than hydride, transfer.[273] A similar argument for promoting motions involved in heavy atom transfer has been made for nucleoside phosphorylase.[288]

Several of the "compensatory mutations" in HIV protease are found in or near regions of above-average ps−ns mobility. These mutations may restore or alter the promoting motions in resistant mutants with reduced catalytic activity. The time-averaged or "ground-state" structures of HIV protease with and without compensatory mutations may be almost identical but differ in their dynamical qualities.[272] This suggests an evolutionary mechanism for drug resistance that is dependent on distal mutations and favorable changes in protein dynamics. There is also potential to use these observations in drug design, either by synthesizing more flexible inhibitors to accommodate heterogeneous receptors or by targeting small molecules against distant parts of the enzyme involved in coordinated movement. The flaps and the dimer interface are attractive targets for inhibitor binding,[270] and NMR has shown both regions to be dynamic on the μs−ms time scale.

3.4. Protein Dynamics during Turnover in Cyclophilin A

Cyclophilin A (CypA) is a peptidyl-prolyl *cis*−*trans* isomerase implicated in a variety of biological reactions such as protein folding and intracellular protein transport.[289−291] It is the major target of the immunosuppressive drug cyclosporin A, although the exact mechanism of action is not yet known.[292] The enzyme is also required for HIV infectivity. CypA is packaged into HIV virions, and NMR studies have shown that CypA can catalyze isomerization of the HIV capsid protein, implying a direct role for CypA in the life cycle of HIV.[293]

The simple nature of the chemical reaction suggests that CypA is a good model system for understanding the connections between structure, function, and protein dynamics, especially in relation to the catalytic step itself.[78] Along these lines, ps−ns and μs−ms time-scale motions were monitored for CypA during enzymatic turnover, using a model peptide as substrate.[294] Variation of the substrate concentration allowed the teasing apart of the motions due to substrate binding/product release and chemical transformation.[294] T_1 and NOE values for the backbone amides did not change appreciably, suggesting little difference in the ps−ns time-scale motions as catalysis proceeds.[294] However, 10 residues showed changes in R_2 values as a function of substrate concentration and were identified as undergoing conformational exchange[294] (Figure 14). The substrate concentration dependence of nine of these residues can be explained purely on the basis of binding events: however, a model encompassing both substrate binding and the isomerization step itself was required to explain the relaxation behavior of Arg55. This suggests that, during chemical

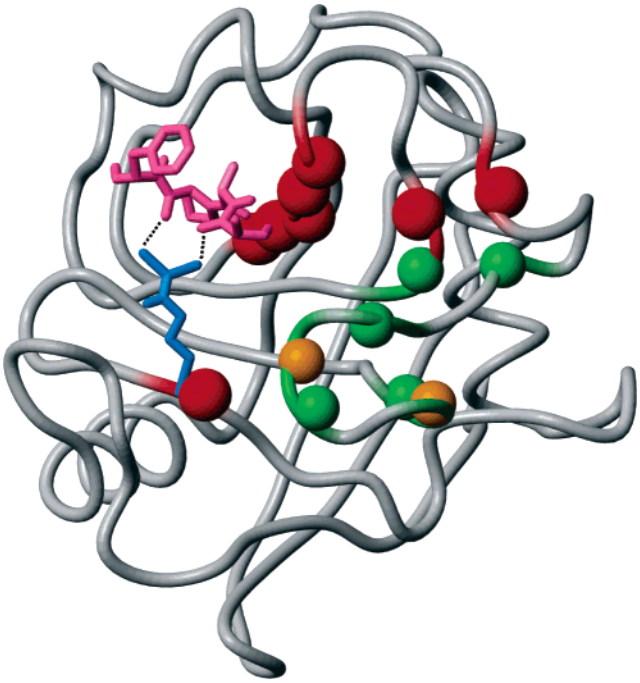

Figure 14. μs−ms time-scale motions in cyclophilin A during turnover (PDB 1RMH). Residues showing increased R_2 during turnover are shown in red, and residues exhibiting conformational exchange in the presence and absence of substrate are shown in green.[294] Residues 68 and 72 (shown in orange) show chemical exchange in the absence of substrate, but an increase in its presence. Hydrogen bonds between Arg55 (blue) and peptide (pink) are shown as dotted lines.

transformation, Arg55 experiences μs−ms time-scale motions on the same time scale as isomerization. Arg55 has been identified as a critical residue for catalysis.[293,295] The side-chain guanidino group of Arg55 is hydrogen bonded to the prolyl nitrogen of the substrate and has been suggested to promote isomerization by weakening the double bond character of the peptide bond[294−297] (Figure 15B). Computer simulations suggest that Arg55 is part of a conserved network of motionally coupled residues extending from surface regions to the active site; this motion is directly implicated in transition-state barrier crossing.[289,298]

The results with CypA stand in stark contrast to what is generally assumed about the rigidness of an enzyme active site during catalysis. In CypA, movement of Arg55 and not rigidity are critical for chemical transformation.[289,294,298] NMR studies in other enzymes, such as α-lytic protease,[299] DNA polymerase β,[300] low molecular weight protein tyrosine phosphatase,[301] binase,[302] and thioesterase/protease I,[303] have also noted μs−ms time-scale motions of catalytically important amino acid residues on the same time scale as chemical transformation. In α-lytic protease, lyophilization induces a conformational change such that His57, an important residue interacting with the catalytic triad of the protease, is less mobile and catalytic activity is reduced.[299] The application of mild pressure reverses the conformational change, increases the mobility of His57, and restores catalytic activity.[299] All of these results point toward a dynamic active site, and computer simulations for a number of enzymes, as discussed above, suggest that these molecular excursions are critically important for catalysis [265,273,288,289]

More quantitative information on μs−ms time-scale motions in CypA with and without substrate was obtained through backbone ^{15}N and side-chain ^{13}C R_2 relaxation

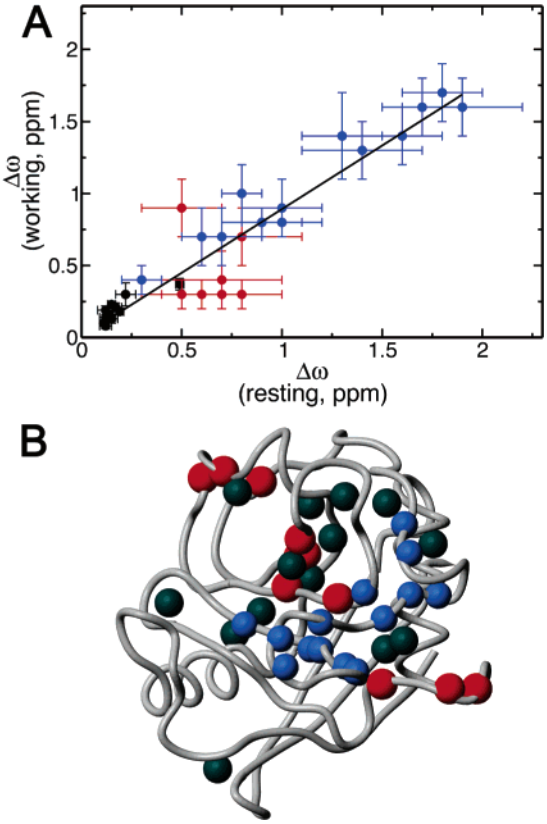

Figure 15. μs−ms time-scale motions in cyclophilin A during rest and turnover. When the enzyme is actively catalyzing *cis*/*trans* isomerization, a single global k_{ex} (2730 s^{-1}) dominates for both ^{15}N backbone (blue and red) and ^{13}C methyl side-chain (black) resonances. Similar residues exhibit conformational exchange in the resting enzyme, but some residues are fit to a global k_{ex} of 1140 s^{-1} (red) and other residues to a k_{ex} of 2260 s^{-1} (blue). (A) The correlation between $\Delta\omega$ values for the resting and working enzymes suggests similar processes, and thus, the "intrinsic dynamics" of CypA are important for catalysis. (B) The residues plotted in panel A are shown as colored balls on the structure of CypA (PDB 1RMH). This figure was generated in part by MOLMOL[354] with data from ref 304.

dispersion experiments.[304] Conformational exchange measured during turnover for both ^{15}N and ^{13}C probes could be fit with a global k_{ex} of 2730 s^{-1}. This value corresponds very well with the sum of the rate constants of *cis*-to-*trans* and *trans*-to-*cis* isomerization (k_{ex} = 2500 s^{-1}), providing further support for intimate links between protein motion and catalysis in CypA.[304] Many of the same regions in the free enzyme experience μs−ms time-scale motions similar to those observed with bound substrate[304] (Figure 15). The majority of the residues could be fit globally to a k_{ex} of 1140 s^{-1}, smaller than what is observed during turnover. Similar to what was observed in RNaseA and DHFR, there was a significant correlation between $\Delta\omega$ and $\Delta\delta$ ($ES_{cis} - ES_{trans}$), suggesting that free CypA exists in a highly skewed and dynamic equilibrium between a "ground-state" and an "excited-state" conformation[304] (Figure 15). Mutational analyses of residues experiencing μs−ms time-scale motions altered the populations of the major and minor substates without significantly affecting either k_{ex} or $\Delta\omega$ values.[304] This analysis included both active-site and distant residues, and while only the active-site mutations affected catalytic activity (k_{cat}/K_m), nearly all mutations reduced substrate affinity.[304] This provides further support to the conformational selection hypothesis outlined above for RNaseA and DHFR. Substrate

binds to a minor protein conformation; reduction of the population of this conformation leads to a decrease in the apparent substrate binding affinity.

It is intriguing that most of the same dynamic processes detected during catalysis are also present in the free enzyme. However, this may not be the case for other enzymes. CypA catalyzes a one-substrate reaction, and its simplicity may not be representative of protein dynamics in more complex systems. Our own studies on DHFR demonstrate that μs−ms time-scale motions are very ligand specific, in marked contrast to what is observed in CypA.[160,205] Detailed studies of additional systems will be needed to determine the general extent of ligand-specific and nonspecific μs−ms time-scale dynamics in enzymes.

3.5. Mesophilic and Thermophilic Enzymes: Adenylate Kinase and Ribonuclease HI

Adenylate kinase (AK) is a ubiquitous enzyme involved in controlling the cellular energy balance by catalyzing the interconversion between ATP/AMP and two ADP molecules.[305] Over 20 crystal structures of the 23.6 kDa enzyme have been solved, and they reveal a very large conformational change as the enzyme progresses through its catalytic cycle.[306,307] The enzyme can be divided into three major domains, the CORE, AMP_{bind}, and LID domains (Figure 4). The AMP_{bind} and LID domains close over the AMP- and ATP-binding sites, respectively, in response to ligand binding (Figure 4). We have already mentioned briefly the studies on the ps−ns time-scale motions of the enzyme from *E.coli*;[169,172] similar motions have been reported for both the *E.coli* and *Mycobacterium tuberculosis* apoenzymes.[308] In the *E. coli* enzyme, there is loss of motion in the flexible AMP_{bind} and LID domains upon binding the two-substrate mimic AP_5A (P^1,P^5-bis(5′-adenosine)pentaphosphate).[169,172] However, there is a corresponding increase in the ps−ns time-scale motions for two loops in the CORE domain that act as an "energetic counterweight" (Figure 4). These CORE domain loops are rigid in the free enzyme, but S^2_{NH} decreases with inhibitor bound.[169,172]

The μs−ms time-scale motions of mesophilic (*E. coli*) and thermophilic (*Aquifex aeolicus*) AKs have been compared during enzymatic turnover, using experiments similar to those performed for CypA.[204] Conformational exchange was detected for residues throughout both proteins (Figure 16), and the relaxation dispersion data for the exchanging residues could be fit with a similar global $k_{ex} \sim 1600-1700$ s^{-1}.[204] The observed correlation between $\Delta\omega$ and $\Delta\delta$(E − E:AMP:AMPPNP) suggests that, in both enzymes, the AMP_{bind} and LID domains open and close over the active-site pocket during catalytic turnover (Figure 16). However, the populations of the ground and excited substates were different for the mesophilic and thermophilic enzymes, resulting in different lid opening rates (k_{open}) at 303 K. In both cases, k_{open} compared favorably to k_{cat}. For *E. coli* AK, the k_{open} derived from R_2 relaxation dispersion experiments was 44 s^{-1} and $k_{cat} \sim 30$ s^{-1}, whereas, for the *A. aeolicus* enzyme, $k_{open} \sim 286$ s^{-1} and $k_{cat} \sim 263$ s^{-1}. This implies that the rate-determining step in AK is lid opening, which is likely an important event in the release of product. Moreover, the differences in the rates for mesophilic and thermophilic AKs can be completely accounted for by slower lid opening in the *A. aeolicus* enzyme.[204] At higher temperature, the thermophilic enzyme exhibits a higher k_{ex} (>10,000 s^{-1} at 333 K) and a corresponding increase in k_{cat}.

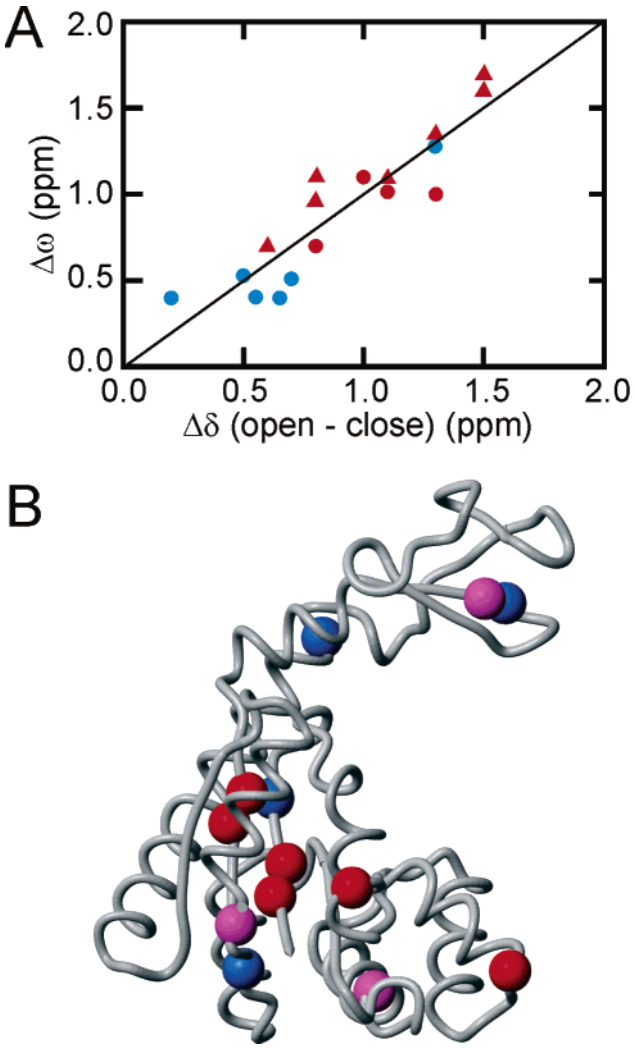

Figure 16. μs−ms time-scale motions reporting on the close−open conformational change in mesophilic *E. coli* (blue) and thermophilic *A. aeolicus* (red) adenylate kinase. (A) The dynamic chemical shift ($\Delta\omega$) changes observed for the ADP (circle) and AMPPNP/AMP (triangle) complexes correlate to an open−close conformational change ($\Delta\delta$). Exchange rate constants in AK correspond to k_{cat}, suggesting that opening of the active-site pocket and product release are rate limiting and that kinetic differences between mesophilic and thermophilic enzymes arise solely due to different lid opening rates. (B) The amide nitrogens whose resonances were used to generate panel A are plotted onto *E. coli* AK (PDB 4AKE), colored red and blue, correspondingly, with magenta balls corresponding to amide nitrogens with both red and blue data points in panel A. The figure was generated in part by MOLMOL[354] with data taken from ref 204.

In AK, as in many other enzymes, the chemical transformation step is not rate limiting. Conformational fluctuations in an enzyme are very often rate limiting, and the rate-determining step frequently involves product release. NMR studies on other enzymes, such as the ribonuclease binase,[302] triosephosphate isomerase,[309,310] and OMP synthase,[311] have also implicated protein dynamics in rate-determining ligand release.

Structures tend to be similar between mesophilic and thermophilic pairs, and important catalytic residues are conserved.[312−314] This suggests that the chemical mechanisms are also very similar, and so, chemistry alone, especially within a static framework, cannot explain the kinetic differences between the enzymes. It has been suggested that homologous enzymes adjust their flexibility to perform

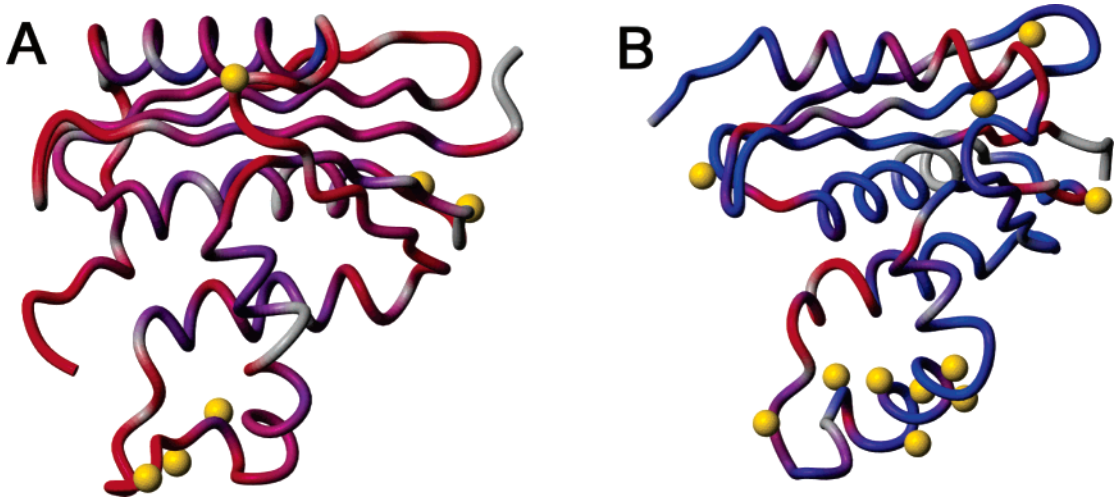

Figure 17. ps−ns and μs−ms time-scale motions in mesophilic and thermophilic ribonuclease HI. S^2_{NH} is color-coded ($S^2 < 0.75$, red, to $S^2 > 0.95$, blue) onto the backbone of (A) *E. coli* RNaseHI (PDB 2RN2) and (B) *T. thermophilus* RNaseHI (PDB 1RIL) at 310 K. Residues with significant conformational exchange are indicated with yellow balls. The mesophilic *E.coli* enzyme tends to show increased ps−ns motions, but the *T. thermophilus* enzyme shows greater μs−ms motions. There are also regions in the thermophilic enzyme that show increased ps−ns motion over that of the mesophilic enzyme. The figure was generated using MOLMOL[354] with data from ref 317.

catalysis at their physiologically relevant temperatures.[315,316] However, more complicated changes in protein dynamics than are observed in AKs may evolve. For instance, a comparison of relaxation parameters between mesophilic and thermophilic ribonuclease HI (RNaseHI) at 310 K demonstrated that more residues in the thermophilic enzyme experience conformational exchange[317,318] (Figure 17). There are also regions in the polypeptide backbone that experience greater ps−ns time-scale motions in the mesophilic enzyme, and other regions where the opposite is true. A temperature titration of the R_{ex} values reveals heightened activation energy barriers for the thermophilic RNaseHI.[317] An increase in energy barrier height would shift the dynamics to a slower time scale, as observed for the thermophilic enzyme. At higher temperatures, these barriers would more readily be overcome, increasing enzyme dynamics that may be important for optimal catalysis.

The results for AK and RNaseHI suggest multiple paths to the same goal of balancing flexibility and function with stability. In AK, the differences in the μs−ms time-scale motions may be traced to the energy differences between the substates, but in RNaseHI, differences may also be attributed to the energy barrier connecting the substates. Further study of psychrophilic−mesophilic−thermophilic enzymes,[316,319] or enzymes found in other extreme environments,[320] can determine to what extent these pathways or alternative pathways determine the connections between flexibility and enzyme function. These mechanistic questions are not merely of academic interest, as many of these "extremozymes" have industrial uses,[321,322] and NMR can play a role in the optimization of these important catalysts.

3.6. Protein Dynamics in Larger Enzymes

The results we have discussed so far have focused on fairly small enzyme systems (<25 kDa). Traditionally, NMR has been size-limited, owing partly to a decrease in sensitivity as R_2 increases as a function of molecular weight. However, newer TROSY techniques are opening the methodology to larger enzyme systems.[62,63,323−326] TROSY operates by selectively recording only the slowly decaying components of the NMR signal. For example, for a ^{1}H−^{15}N pair, the ^{1}H NMR signal is a doublet, with the two resonance lines representing ^{1}H coupled to "spin up" and "spin down" ^{15}N. The signals are normally collapsed by "decoupling", and the relaxation rates for the two resonances are averaged. However, the multiplet components have different relaxation rates; TROSY experiments select exclusively the slower decaying resonance. This can lead to a decrease in signal intensity for smaller proteins, but the favorable relaxation rate more than compensates for this loss in larger proteins.[62] The technique is especially suitable for proteins with molecular mass greater than 15−20 kDa at field strengths greater than 700 MHz (^{1}H).

TROSY techniques have been applied to study both ps−ns and μs−ms time scale motions of malate synthase G (MSG),[64] an 82-kDa enzyme that catalyzes the Claisen condensation of glyoxylate with an acetyl group from acetyl-CoA to produce malate.[327,328] MSG is a potential target for antimicrobial agents.[328] The structure of MSG has been determined in complex with glyoxylate[328] and in an abortive ternary complex with pyruvate (glyoxylate mimic) and acetyl-CoA (AcCoA)[329] by X-ray crystallography, and more recently, the ligand-free structure has been solved by solution NMR.[330] There are four major domains of the enzyme, including the "core" composed of a parallel, eight-stranded β-sheet surrounded by eight α-helices, an α-helical "clasp" in the N-terminus, an α/β domain appended to the core, and a C-terminus five-helix "plug"[330] (Figure 18). A comparison between the apoenzymes and ligand-bound enzymes did not reveal any major conformational rearrangement upon binding substrate.[330]

NMR studies have focused on ps−ns and μs−ms side-chain motions of MSG. Several methyl groups with decreased S^2_{axis} values have been identified in the apoenzyme, including residues in the α/β domain (Val155, Ile309, and Val310), in the linker between the core and the C-terminal plug (Val556 and Leu581), and in the loops connecting the four domains (Leu91, Val92, Ile260, and Ile265).[327] Many of these side chains are at the active-site binding interface, and not surprisingly, S^2_{axis} increases in the ternary E:pyruvate:AcCoA complex[327] (Figure 18). This is partially compensated by small decreases in S^2_{axis} values for other methyl sites (Figure 18), although calculations suggest an overall loss of

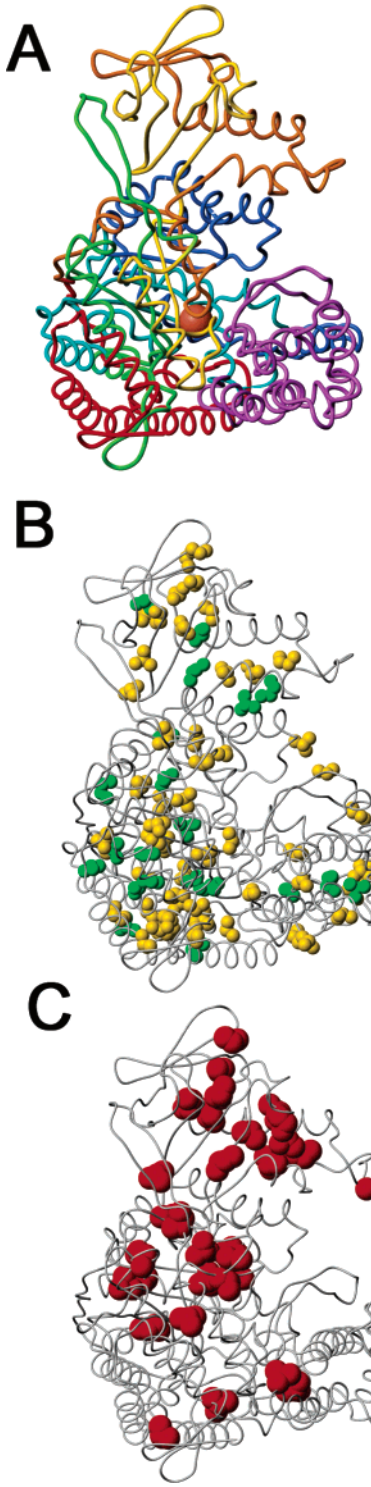

Figure 18. Side-chain methyl dynamics of the 82 kDa enzyme malate synthase G. (A) Ribbon diagram of the glyoxylate-bound enzyme (PDB 1D8C), color coded from red at the N-terminus through orange, yellow, green, and blue to purple at the C-terminus. (B) Comparison of ps−ns time-scale methyl dynamics between free and ternary (E:pyruvate:acetyl CoA) enzyme using ^{13}C and ^{2}H probes. Residues with increased ps−ns motion in the ternary enzyme (i.e. $S^2_{free} > S^2_{ternary}$) are colored green, and residues with decreased ps−ns time-scale motion in the ternary enzyme (i.e. $S^2_{free} < S^2_{ternary}$) are colored yellow. Differences were deemed significant if $|S^2_{free} - S^2_{ternary}| > 0.02$ and there was no disagreement between ^{2}H and ^{13}C probes. (C) Residues with significant ^{13}C-methyl R_{ex} in the free enzyme are colored red. The figure was generated using MOLMOL[354] using data from ref 331.

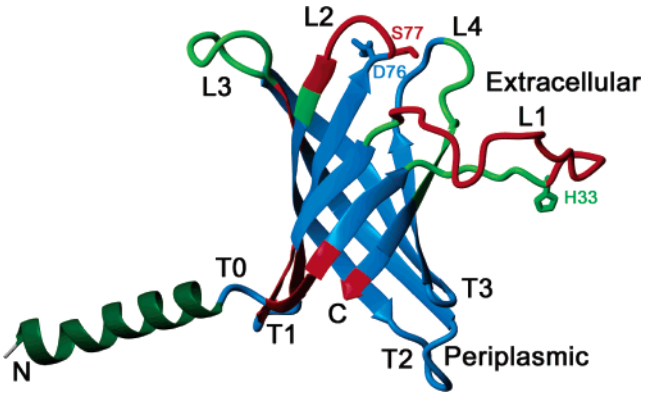

Figure 19. Motions in the integral membrane enzyme PagP detected with solution NMR. Residues colored in red have backbone ^{15}N T_1's that are less than 80% of the value predicted for a 20-ns overall correlation time, $S^2 = 0.85$, $\tau_e = 10$ ps (i.e. 2.3 s). His 33 has NMR signals too faint to be detected in $^{1}H-^{15}N$ HSQC spectra; other green residues have a weak but observable signal. All other residues are shown in blue. Reprinted with permission from ref 326. Copyright 2002 National Academy of Sciences, U.S.A.

53 J mol^{-1} K^{-1} in entropy from the free enzyme.[327] Comparisons of the μs−ms time-scale motions in the free and ternary enzymes are not available, but backbone (^{15}N) and side-chain (^{13}C) R_2 relaxation dispersion studies on the apoenzyme have also indicated that the binding pocket is flexible on this slower time scale.[331] R_{ex} contributions were observed throughout the enzyme, with the most significant conformational exchange occurring in the core and α/β domains, and the smallest μs−ms time-scale motions in the C-terminal domain and the N-terminal clasp[331] (Figure 18). This is intriguing in light of the fact that the relative orientation of the domains does not change upon ligand binding, in contrast to what is observed in structurally and functionally similar enzymes.[328,332] Transient sampling of higher energy conformations and/or altered protein dynamics may perform the same functional role in MSG as gross structural changes, required for substrate binding and/or product release, do in related enzymes.

TROSY methods have also been applied to integral membrane proteins.[323,325,326] In particular, the solution structure and dynamics of the bacterial outer membrane enzyme PagP, which transfers a palmitate chain from a phospholipid to lipid A, have been studied in micelles (50−60 kDa).[326] The core of the protein consists of an eight-stranded antiparallel β-barrel with an amphipathic helix and disordered solvent exposed loops[326] (Figure 19). The loops are exceptionally mobile on the ps−ns time scale, as evidenced by increased R_1 values (Figure 19).[326] ^{15}N R_2 relaxation dispersion experiments also indicate that the loops, especially the large L1 loop connecting strands A and B, experience μs−ms time-scale motions[333] (Figure 19). When the temperature is lowered, new HSQC peaks appear and directly confirm the presence of a minor conformer.[333] The higher energy conformation may be important in substrate access or ligand regress, as discussed above for other enzymes.

The largest enzyme that has been studied by NMR is the 300-kDa cylindrical protease ClpP.[65] ClpP functions as a double heptamer with the catalytic sites located in the interior (Figure 20). Proteins marked for degradation are unfolded and threaded through the axial pores by the chaperones ClpX and ClpA.[334−336] However, the path by which products escape was not previously known. ^{13}C methyl R_2 relaxation dispersion experiments indicated that the side chains of Ile149 and

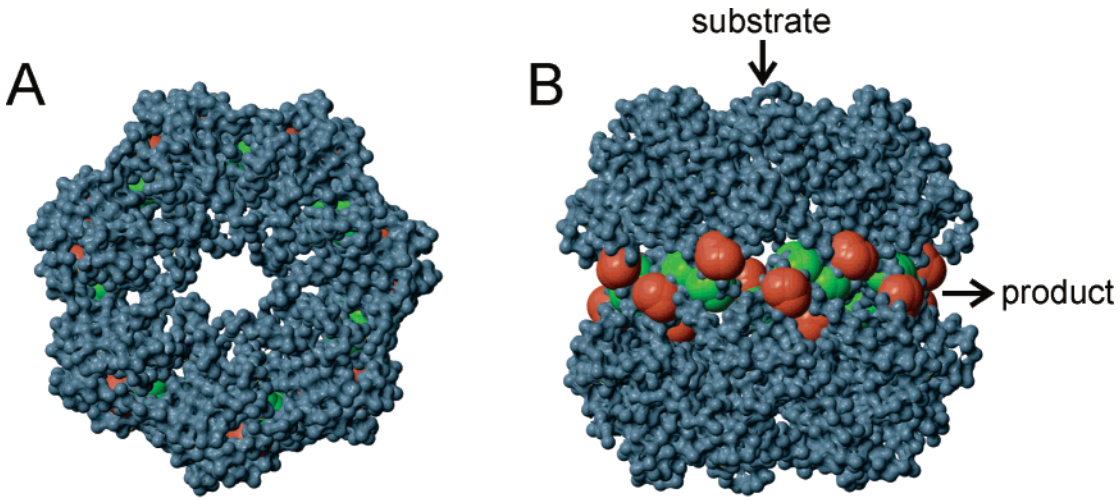

Figure 20. Dynamic side pores in ClpP protease (PDB 1TYF). (A) Surface representation of the top view showing the entrance channel to the catalytic interior. Chaperones guide the protein substrate through the channel. (B) Side view showing the potential product release route at the interface between the two heptameric rings. Ile149 and Ile151 (Ile135 and Ile137 according to the PDB numbering), that were shown to be dynamic on the μs−ms time scale, are shown in green and orange, respectively.[65]

Ile151 are flexible on the μs−ms time scale (Figure 20). The relaxation dispersion data could be fit with a global k_{ex} of 61 s^{-1} at a temperature of $\sim$ 274 K. All residues displayed the same temperature dependence, from which an activation enthalpy and entropy of 13.1 kcal/mol and −3.6 cal mol^{-1} K^{-1}, respectively, were derived.[65] Ile149 and Ile151 are located at the interface between the two heptamer rings of ClpP, and it was suggested the observed μs−ms time-scale motions are involved in product release[65] (Figure 20). To test this mechanism, disulfide bridges were introduced to bond the two rings together. Under reducing conditions, ClpP is functional, but under oxidizing conditions, activity is completely abrogated, even though peptide is retained by the enzyme.[65] These results suggest that the higher energy conformer supplies an escape route for the degradation products without interfering with further substrate entrance, directly connecting protein dynamics to product release in ClpP.

Many enzymes are multidomain proteins composed of both regulatory and catalytic subunits. We have outlined how protein dynamics can affect events throughout the catalytic cycle, including substrate binding, chemical transformation, and product release. Considering the importance of protein dynamics to enzyme function, regulatory units may affect catalytic subunits not only structurally but also dynamically. Communication and interactions in multi-enzyme complexes (e.g. "substrate channeling") are also critically dependent on motion.[337,338] TROSY techniques, together with "isotopic segmental labeling" that can both reduce spectral complexity and provide focus on the protein domain of interest,[339−342] promise to make studies of the dynamics of these complex enzyme systems tractable by NMR.

4. Conclusions

NMR relaxation techniques have been used to study multiple time-scale dynamics of enzymes in different phases of the catalytic cycle. These studies suggest that protein motion plays important roles in all aspects of catalysis. Catalysis and ligand exchange generally occur on the μs−ms time scale that corresponds to the time domain of protein conformational change, suggesting that conformational change is intimately related to these enzymatic events. This has generally been taken as support for the "induced-fit" hypothesis; ligand binds to one conformation, and this interaction pushes the enzyme into an alternative conformation that forms more favorable interactions with the ligand.[343] However, for this process to occur, the ligand must have some affinity for the initially encountered protein conformation, and it is not always apparent from apoenzyme structures how this might transpire. This is underscored by, for example, ligand binding to the cavity mutant of T4 lysozyme, where it is not at all clear how the ligand would form an initial favorable complex with the enzyme. Whereas the induced-fit mechanism assumes conformational *homogeneity*, conformational selection takes account of the fact that proteins may adopt an ensemble of conformations; i.e., they are *heterogeneous* in conformation.[83,223−229] Thus, an enzyme may consist of a major conformer, comprising >90% of the molecules in the ensemble, yet it is one of the minor conformers that interacts with the ligand (Figure 9). Ligand binding then decreases ΔG for the complex, and the bound conformation becomes more highly populated in the ensemble. This implies that the enzyme exists as an ensemble of interconverting conformational states and that ligand binding merely changes the conformational equilibrium.[228]

Substrate binding, product release, and chemical transformation can all affect the conformational equilibrium.[83] RNase A, for example, can exist in solution in at least two conformations, representing the free and bound forms of the enzyme.[206,230] Substrate can bind to a protein conformation resembling the lowest energy conformation of the bound form, and product may be released from a higher energy conformation that is structurally similar to the lowest energy conformation of the free form. Similar processes are apparent in adenylate kinase (AK) where the product release rate constant corresponds to the rate constant for the lower-to-higher energy conformational transition determined by R_2 relaxation dispersion.[204] The model Michaelis complex for DHFR (E:$NADP^+$:folate) is also in conformational equilibrium between a "*closed*" substrate conformation and a product "*occluded*" conformation.[205] Our unpublished results suggest analogous processes are occurring throughout the catalytic cycle of DHFR.

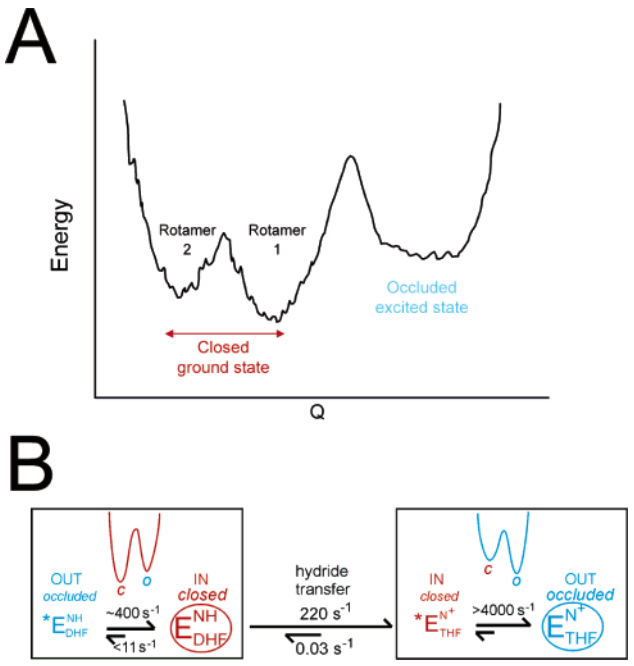

Figure 21. Energy landscape of dihydrofolate reductase in the Michaelis model complex E:NADP$^+$:folate. (A) The ground-state conformation of E:NADP$^+$:folate is *closed*. Within the *closed* ground state, side chain coupling constant measurements reveal the existence of two substates that differ in the rotamer populations of certain aliphatic side chains. R_2 relaxation dispersion experiments have also identified a higher energy *occluded* conformation. (B) Dynamic energy landscape of DHFR. The ground-state conformation of the Michaelis complex (E:DHF:NADPH) is *closed*. Following the chemical step, the energy landscape changes: the *closed* state in which hydride transfer occurs is now a higher energy state of the E:THF:NADP$^+$ product, which relaxes rapidly to the new *occluded* ground state. Panel B is reproduced with permission from ref 205. Copyright 2005 National Academy of Sciences, U.S.A.

Enzymes thus represent *dynamic* energy landscapes.[83] The binding of substrate, release of products, and substrate-to-product conversion will affect the relative energies of the various substates. The energy landscape shifts in response to the presence of ligands, and these shifts, in turn, guide the enzyme further along its catalytic cycle.[83] Mutations or allosteric inhibitors affecting the energy landscape will thus generally have a detrimental impact on catalysis.[175,344]

Larger barrier heights lead to longer time-scale motions. The ps−ns time-scale motions reflect crossing of the smaller barriers and are determined by the "ruggedness" of the energy landscape. Slower time-scale motions can be attributed to larger barriers and represent "true" conformational transitions between substates. In RNaseHI, the barriers in the energy landscape for the thermophilic enzyme are larger, and hence, motions are reduced on the ps−ns time scale but are increased on the μs−ms time scale compared to the case of the mesophilic protein.[317] In DHFR, the energy landscape for the E:NADP$^+$:folate complex consists of the ps−ns time-scale ruggedness, the *trans*−*gauche* rotameric substates in the *closed* conformation, and a higher energy *occluded* conformation (Figure 21). The rotameric substates in DHFR may be important for transition-state stabilization. Following hydride transfer, the now higher-energy *closed* conformation must then collapse into a lower-energy *occluded* conformation in the E:THF:NADP$^+$ product complex.

The results from NMR studies may hide even further complexity. NMR is an ensemble technique, and the observed higher energy conformations may themselves give a time-averaged view of the energy landscape. Single molecule studies have shown that individual enzymes do not perform catalysis at identical rates, and turnover fluctuates even in the same enzyme molecule.[345−353] The individual enzymes may be following different paths through the dynamic energy landscape, analogous to following different folding paths to the same globular structure, that are governed by Boltzmann probability and individual kinetic energies. This view also suggests that there is not a single transition state relevant to chemical transformation but that there are multiple paths to product. This scheme is much more complicated than the traditional one-dimensional reaction coordinate, but as discussed, this provides a framework for understanding diverse topics such as ligand exchange, allostery, protein stability in mesophiles/thermophiles, enthalpy−entropy compensation, and kinetic heterogeneity.

It is now clear that we are moving past a static view of proteins and enzyme catalysis. NMR will undoubtedly continue to provide fundamental insight into enzyme dynamics and provide the necessary experimental evidence to test theories of catalysis.

5. Acknowledgment

We thank current and former members of the Wright−Dyson research group for insightful discussions. This work was supported by Grants GM56879 and GM75995 from the National Institutes of Health.

6. References

(1) Hammes, G. G. *Biochemistry* **2002**, *41*, 8221.
(2) Gutteridge, A.; Thornton, J. *J. Mol. Biol.* **2005**, *346*, 21.
(3) Gutteridge, A.; Thornton, J. *FEBS Lett.* **2004**, *567*, 67.
(4) Yon, J. M.; Perahia, D.; Ghelis, C. *Biochimie* **1998**, *80*, 33.
(5) Schnell, J. R.; Dyson, H. J.; Wright, P. E. *Annu. Rev. Biophys. Biomol. Struct.* **2004**, *33*, 119.
(6) Guallar, V.; Jacobson, M.; McDermott, A.; Friesner, R. A. *J. Mol. Biol.* **2004**, *337*, 227.
(7) Williams, J. C.; McDermott, A. E. *Biochemistry* **1995**, *34*, 8309.
(8) Taylor, S. S.; Yang, J.; Wu, J.; Haste, N. M.; Radzio-Andzelm, E.; Anand, G. *Biochim. Biophys. Acta* **2004**, *1697*, 259.
(9) Yang, L. W.; Bahar, I. *Structure* **2005**, *13*, 893.
(10) Cannon, W. R.; Singleton, S. F.; Benkovic, S. J. *Nat. Struct. Biol.* **1996**, *3*, 821.
(11) Benkovic, S. J.; Hammes-Schiffer, S. *Science* **2003**, *301*, 1196.
(12) Rajagopalan, P. T.; Benkovic, S. J. *Chem. Rec.* **2002**, *2*, 24.
(13) Knapp, M. J.; Klinman, J. P. *Eur. J Biochem.* **2002**, *269*, 3113.
(14) Daniel, R. M.; Dunn, R. V.; Finney, J. L.; Smith, J. C. *Annu. Rev. Biophys. Biomol. Struct.* **2003**, *32*, 69.
(15) Sutcliffe, M. J.; Scrutton, N. S. *Trends Biochem. Sci.* **2000**, *25*, 405.
(16) Wand, A. J. *Nat. Struct. Biol.* **2001**, *8*, 926.
(17) Antoniou, D.; Caratzoulas, S.; Kalyanaraman, C.; Mincer, J. S.; Schwartz, S. D. *Eur. J. Biochem.* **2002**, *269*, 3103.
(18) Tousignant, A.; Pelletier, J. N. *Chem. Biol.* **2004**, *11*, 1037.
(19) Mulder, F. A.; Mittermaier, A.; Hon, B.; Dahlquist, F. W.; Kay, L. E. *Nat. Struct. Biol.* **2001**, *8*, 932.
(20) Mittermaier, T.; Mulder, F.; Dahlquist, R.; Kay, L. E. *Sci. World J.* **2002**, *2*, 45.
(21) Kay, L. E. *Nat. Struct. Biol.* **1998**, *5*, 513.
(22) Wang, C.; Palmer, A. G., III. *Magn. Reson. Chem.* **2003**, *41*, 866.
(23) Stevens, R. C.; Yokoyama, S.; Wilson, I. A. *Science* **2001**, *294*, 89.
(24) Prestegard, J. H.; Valafar, H.; Glushka, J.; Tian, F. *Biochemistry* **2001**, *40*, 8677.
(25) Brenner, S. E. *Nat. Rev. Genet.* **2001**, *2*, 801.
(26) Hilvert, D. *Annu. Rev. Biochem.* **2000**, *69*, 751.
(27) Bolon, D. N.; Voigt, C. A.; Mayo, S. L. *Curr. Opin. Chem. Biol.* **2002**, *6*, 125.
(28) Ueba, H.; Wolf, M. *Science* **2005**, *310*, 1774.
(29) Johanek, V.; Laurin, M.; Grant, A. W.; Kasemo, B.; Henry, C. R.; Libuda, J. *Science* **2004**, *304*, 1639.
(30) Hansen, P. L.; Wagner, J. B.; Helveg, S.; Rostrup-Nielsen, J. R.; Clausen, B. S.; Topsoe, H. *Science* **2002**, *295*, 2053.
(31) Teague, S. J. *Nat. Rev. Drug Discovery* **2003**, *2*, 527.

(32) Williams, D. H.; Stephens, E.; Zhou, M.; Zerella, R. *Methods Enzymol.* **2004**, *380*, 3.
(33) Murphy, K. P. *Med. Res. Rev.* **1999**, *19*, 333.
(34) Homans, S. W. *ChemBioChem* **2005**, *6*, 1585.
(35) Eletsky, A.; Kienhofer, A.; Hilvert, D.; Pervushin, K. *Biochemistry* **2005**, *44*, 6788.
(36) Davis, J. H.; Agard, D. A. *Biochemistry* **1998**, *37*, 7696.
(37) Yu, L.; Zhu, C. X.; Tse-Dinh, Y. C.; Fesik, S. W. *Biochemistry* **1996**, *35*, 9661.
(38) Roberts, G. C. K. *Curr. Opin. Biotechnol.* **1999**, *10*, 42.
(39) Gane, P. J.; Dean, P. M. *Curr. Opin. Struct. Biol.* **2000**, *10*, 401.
(40) Homans, S. W. *Angew. Chem., Int. Ed. Engl.* **2004**, *43*, 290.
(41) McCammon, J. A.; Harvey, S. C. *Dynamics of Proteins and Nucleic Acids*; Cambridge University Press: Cambridge, 1987.
(42) Palmer, A. G. *Annu. Rev. Biophys. Biomol. Struct.* **2001**, *30*, 129.
(43) Doniach, S. *Chem. Rev.* **2001**, *101*, 1763.
(44) Zaccai, G. *Science* **2000**, *288*, 1604.
(45) Weiss, S. *Nat. Struct. Biol.* **2000**, *7*, 724.
(46) Yang, H.; Luo, G.; Karnchanaphanurach, P.; Louie, T. M.; Rech, I.; Cova, S.; Xun, L.; Xie, X. S. *Science* **2003**, *302*, 262.
(47) Haustein, E.; Schwille, P. *Curr. Opin. Struct. Biol.* **2004**, *14*, 531.
(48) Wales, T. E.; Engen, J. R. *Mass Spectrom. Rev.* **2006**, *25*, 158.
(49) Busenlehner, L. S.; Armstrong, R. N. *Arch. Biochem. Biophys.* **2005**, *433*, 34.
(50) Guan, J. Q.; Chance, M. R. *Trends Biochem. Sci.* **2005**, *30*, 583.
(51) Talkington, M. W.; Siuzdak, G.; Williamson, J. R. *Nature* **2005**, *438*, 628.
(52) Engler, N.; Ostermann, A.; Niimura, N.; Parak, F. G. *Proc. Natl. Acad. Sci., U.S.A.* **2003**, *100*, 10243.
(53) Parak, F. G. *Curr. Opin. Struct. Biol.* **2003**, *13*, 552.
(54) Thomas, G. J., Jr. *Annu. Rev. Biophys. Biomol. Struct.* **1999**, *28*, 1.
(55) Zanni, M. T.; Hochstrasser, R. M. *Curr. Opin. Struct. Biol.* **2001**, *11*, 516.
(56) Barth, A.; Zscherp, C. *FEBS Lett.* **2000**, *477*, 151.
(57) Karplus, M.; Kuriyan, J. *Proc. Natl. Acad. Sci. U.S.A.* **2005**, *102*, 6679.
(58) Hansson, T.; Oostenbrink, C.; van Gunsteren, W. *Curr. Opin. Struct. Biol.* **2002**, *12*, 190.
(59) Bahar, I.; Rader, A. J. *Curr. Opin. Struct. Biol.* **2005**, *15*, 586.
(60) Goto, N. K.; Kay, L. E. *Curr. Opin. Struct. Biol.* **2000**, *10*, 585.
(61) Riek, R.; Fiaux, J.; Bertelsen, E. B.; Horwich, A. L.; Wuthrich, K. *J. Am. Chem. Soc.* **2002**, *124*, 12144.
(62) Fernandez, C.; Wider, G. *Curr. Opin. Struct. Biol.* **2003**, *13*, 570.
(63) Fiaux, J.; Bertelsen, E. B.; Horwich, A. L.; Wuthrich, K. *Nature* **2002**, *418*, 207.
(64) Tugarinov, V.; Hwang, P. M.; Kay, L. E. *Annu. Rev. Biochem.* **2004**, *73*, 107.
(65) Sprangers, R.; Gribun, A.; Hwang, P. M.; Houry, W. A.; Kay, L. E. *Proc. Natl. Acad. Sci., U.S.A.* **2005**, *102*, 16678.
(66) Bryant, J. E.; Lecomte, J. T.; Lee, A. L.; Young, G. B.; Pielak, G. J. *Biochemistry* **2005**, *44*, 9275.
(67) Reckel, S.; Lohr, F.; Dotsch, V. *ChemBioChem* **2005**, *6*, 1601.
(68) Vallurupalli, P.; Kay, L. E. *J Am. Chem. Soc.* **2005**, *127*, 6893.
(69) Latham, M. P.; Brown, D. J.; McCallum, S. A.; Pardi, A. *ChemBioChem* **2005**, *6*, 1492.
(70) Hoogstraten, C. G.; Wank, J. R.; Pardi, A. *Biochemistry* **2000**, *39*, 9951.
(71) Hoogstraten, C. G.; Legault, P.; Pardi, A. *J. Mol. Biol.* **1998**, *284*, 337.
(72) Ishima, R.; Torchia, D. A. *Nat. Struct. Biol.* **2000**, *7*, 740.
(73) Palmer, A. G.; Williams, J.; McDermott, A. *J. Phys. Chem.* **1996**, *100*, 13293.
(74) Palmer, A. G.; Kroenke, C. D.; Loria, J. P. *Methods Enzymol.* **2001**, *339*, 204.
(75) Palmer, A. G. *Curr. Opin. Struct. Biol.* **1997**, *7*, 732.
(76) Palmer, A. G. *Curr. Opin. Biotechnol.* **1993**, *4*, 385.
(77) Kay, L. E. *J. Magn. Reson.* **2005**, *173*, 193.
(78) Kern, D.; Eisenmesser, E. Z.; Wolf-Watz, M. *Methods Enzymol.* **2005**, *394*, 507.
(79) Palmer, A. G., III. *Chem. Rev.* **2004**, *104*, 3623.
(80) Bryngelson, J. D.; Wolynes, P. G. *J. Phys. Chem.* **1989**, *93*, 6902.
(81) Lazaridis, T.; Karplus, M. *Science* **1997**, *278*, 1928.
(82) Frauenfelder, H.; Sligar, S. G.; Wolynes, P. G. *Science* **1991**, *254*, 1598.
(83) Kumar, S.; Ma, B. Y.; Tsai, C. J.; Sinha, N.; Nussinov, R. *Protein Sci.* **2000**, *9*, 10.
(84) Ma, B.; Kumar, S.; Tsai, C. J.; Nussinov, R. *Protein Eng., Des. Sel.* **1999**, *12*, 713.
(85) Tsai, C. J.; Kumar, S.; Ma, B. Y.; Nussinov, R. *Protein Sci.* **1999**, *8*, 1181.
(86) Freire, E. *Proc. Natl. Acad. Sci., U.S.A.* **1999**, *96*, 10118.
(87) Tsai, C. J.; Ma, B.; Nussinov, R. *Proc. Natl. Acad. Sci., U.S.A.* **1999**, *96*, 9970.
(88) Allerhand, A.; Doddrell, D.; Glushko, V.; Cochran, D. W.; Wenkert, E.; Lawson, P. J.; Gurd, F. R. N. *J. Am. Chem. Soc.* **1971**, *93*, 554.
(89) Nigen, A. M.; Keim, P.; Marshall, R. C.; Morrow, J. S.; Gurd, F. R. *J. Biol. Chem.* **1972**, *247*, 4100.
(90) Glushko, V.; Lawson, P. J.; Gurd, F. R. *J. Biol. Chem.* **1972**, *247*, 3176.
(91) Jones, W. C.; Rothgeb, T. M.; Gurd, F. R. N. *J. Biol. Chem.* **1976**, *251*, 7452.
(92) Wittebort, R. J.; Rothgeb, T. M.; Szabo, A.; Gurd, F. R. N. *Proc. Natl. Acad. Sci., U.S.A.* **1979**, *76*, 1059.
(93) Hughes, L. T.; Cohen, J. S.; Szabo, A.; Niu, C.-H.; Matsuura, S. *Biochemistry* **1984**, *23*, 4390.
(94) Campbell, I. D.; Dobson, C. M.; Williams, R. J. P. *Biochem. J.* **1985**, *231*, 1.
(95) McIntosh, L. P.; Griffey, R. H.; Muchmore, D. C.; Nielson, C. P.; Redfield, A. G.; Dahlquist, F. W. *Proc. Natl. Acad. Sci., U.S.A.* **1987**, *84*, 1244.
(96) Kay, L. E.; Jue, T. L.; Bangerter, B.; Demou, P. C. *J. Magn. Reson.* **1987**, *73*, 558.
(97) Sklenár, V.; Torchia, D.; Bax, A. *J. Magn. Reson.* **1987**, *73*, 375.
(98) Nirmala, N. R.; Wagner, W. *J. Am. Chem. Soc.* **1988**, *110*, 7557.
(99) Kay, L. E.; Torchia, D. A.; Bax, A. *Biochemistry* **1989**, *28*, 8972.
(100) McIntosh, L. P.; Dahlquist, F. W. *Q. Rev. Biophys.* **1990**, *23*, 1.
(101) Palmer, A. G.; Rance, M.; Wright, P. E. *J. Am. Chem. Soc.* **1991**, *113*, 4371.
(102) Nicholson, L. K.; Kay, L. E.; Baldisseri, D. M.; Arango, J.; Young, P. E.; Bax, A.; Torchia, D. A. *Biochemistry* **1992**, *31*, 5253.
(103) Kay, L. E. *Prog. Biophys. Mol. Biol.* **1995**, *63*, 277.
(104) Muhandiram, D. R.; Yamazaki, T.; Sykes, B. D.; Kay, L. E. *J. Am. Chem. Soc.* **1995**, *117*, 11536.
(105) Rosen, M. K.; Gardner, K. H.; Willis, R. C.; Parris, W. E.; Pawson, T.; Kay, L. E. *J. Mol. Biol.* **1996**, *263*, 627.
(106) Lee, A. L.; Urbauer, J. L.; Wand, A. J. *J. Biomol. NMR* **1997**, *9*, 437.
(107) Sattler, M.; Schleucher, J.; Griesinger, C. *Prog. Nucl. Magn. Reson. Spectrosc.* **1999**, *34*, 93.
(108) Rozovsky, S.; Jogl, G.; Tong, L.; McDermott, A. E. *J. Mol. Biol.* **2001**, *310*, 271.
(109) Seifert, M. H.; Breitenlechner, C. B.; Bossemeyer, D.; Huber, R.; Holak, T. A.; Engh, R. A. *Biochemistry* **2002**, *41*, 5968.
(110) Gardner, K. H.; Kay, L. E. *Annu. Rev. Biophys. Biomol. Struct.* **1998**, *27*, 357.
(111) LeMaster, D. M.; Kushlan, D. M. *J. Am. Chem. Soc.* **1996**, *118*, 9255.
(112) Wand, A. J.; Bieber, R. J.; Urbauer, J. L.; McEvoy, R. P.; Gan, Z. *J. Magn. Reson., Ser. B* **1995**, *108*, 173.
(113) Ishima, R.; Louis, J. M.; Torchia, D. *J. Am. Chem. Soc.* **1999**, *121*, 1.
(114) Ollerenshaw, J.; Tugarinov, V.; Skrynnikov, N.; Kay, L. *J. Biomol. NMR* **2005**, *33*, 25.
(115) Teilum, K.; Brath, U.; Lundstrom, P.; Akke, M. *J Am. Chem. Soc.* **2006**, *128*, 2506.
(116) Wood, M. J.; Komives, E. A. *J. Biomol. NMR* **1999**, *13*, 149.
(117) Lipari, G.; Szabo, A. *J. Am. Chem. Soc.* **1982**, *104*, 4546.
(118) Lipari, G.; Szabo, A. *J. Am. Chem. Soc.* **1982**, *104*, 4559.
(119) Brüschweiler, R.; Wright, P. E. *J. Am. Chem. Soc.* **1994**, *116*, 8426.
(120) Tugarinov, V.; Liang, Z. C.; Shapiro, Y. E.; Freed, J. H.; Meirovitch, E. *J. Am. Chem. Soc.* **2001**, *123*, 3055.
(121) Schurr, J. M.; Babcock, H. P.; Fujimoto, B. S. *J. Magn. Reson., Ser. B* **1994**, *105*, 211.
(122) Tjandra, N.; Feller, S. E.; Pastor, R. W.; Bax, A. *J. Am. Chem. Soc.* **1995**, *117*, 12562.
(123) Zheng, Z.; Czaplicki, J.; Jardetzky, O. *Biochemistry* **1995**, *34*, 5212.
(124) Fushman, D.; Cahill, S.; Cowburn, D. *J. Mol. Biol.* **1997**, *266*, 173.
(125) Osborne, M. J.; Wright, P. E. *J. Biomol. NMR* **2001**, *19*, 209.
(126) Clore, G. M.; Szabo, A.; Bax, A.; Kay, L. E.; Driscoll, P. C.; Gronenborn, A. M. *J. Am. Chem. Soc.* **1990**, *112*, 4989.
(127) Kördel, J.; Skelton, N. J.; Akke, M.; Palmer, A. G.; Chazin, W. J. *Biochemistry* **1992**, *31*, 4856.
(128) Peng, J. W.; Wagner, G. *Biochemistry* **1995**, *34*, 16733.
(129) Andrec, M.; Montelione, G. T.; Levy, R. M. *J. Magn. Reson.* **1999**, *139*, 408.
(130) Wang, T.; Cai, S.; Zuiderweg, E. R. *J Am. Chem. Soc.* **2003**, *125*, 8639.
(131) Fischer, M. W.; Zeng, L.; Majumdar, A.; Zuiderweg, E. R. *Proc. Natl. Acad. Sci., U.S.A.* **1998**, *95*, 8016.
(132) Pang, Y.; Buck, M.; Zuiderweg, E. R. *Biochemistry* **2002**, *41*, 2655.
(133) Yang, D.; Kay, L. E. *J. Magn. Reson., Ser. B* **1996**, *110*, 213.
(134) Millet, O.; Muhandiram, D. R.; Skrynnikov, N. R.; Kay, L. E. *J. Am. Chem. Soc.* **2002**, *124*, 6439.
(135) Skrynnikov, N. R.; Millet, O.; Kay, L. E. *J. Am. Chem. Soc.* **2002**, *124*, 6449.
(136) Wand, A. J.; Urbauer, J. L.; McEvoy, R. P.; Bieber, R. J. *Biochemistry* **1996**, *35*, 6116.

(137) Mittermaier, A.; Kay, L. E.; Forman-Kay, J. D. *J. Biomol. NMR* **1999**, *13*, 181.
(138) Schnell, J. R.; Dyson, H. J.; Wright, P. E. *Biochemistry* **2004**, *43*, 374.
(139) Goodman, J. L.; Pagel, M. D.; Stone, M. J. *J. Mol. Biol.* **2000**, *295*, 963.
(140) Zhang, F.; Brüschweiler, R. *J. Am. Chem. Soc.* **2002**, *124*, 12654.
(141) Abergel, D.; Bodenhausen, G. *J Chem. Phys.* **2005**, *123*, 204901.
(142) Ming, D.; Brüschweiler, R. *J. Biomol. NMR* **2004**, *29*, 363.
(143) Mittermaier, A.; Davidson, A. R.; Kay, L. E. *J. Am. Chem. Soc.* **2003**, *125*, 9004.
(144) Doig, A. J.; Sternberg, M. J. E. *Protein Sci.* **1995**, *4*, 2247.
(145) Chellgren, B. W.; Creamer, T. P. *Proteins* **2006**, *62*, 411.
(146) Pappu, R. V.; Srinivasan, R.; Rose, G. D. *Proc. Natl. Acad. Sci., U.S.A.* **2000**, *97*, 12565.
(147) Wong, K. B.; Daggett, V. *Biochemistry* **1998**, *37*, 11182.
(148) Forman-Kay, J. D. *Nat. Struct. Biol.* **1999**, *6*, 1086.
(149) Akke, M.; Brüschweiler, R.; Palmer, A. G. *J. Am. Chem. Soc.* **1993**, *115*, 9832.
(150) Wrabl, J. O.; Shortle, D.; Woolf, T. B. *Proteins* **2000**, *38*, 123.
(151) LeMaster, D. M. *J. Am. Chem. Soc.* **1999**, *121*, 1726.
(152) Yang, D.; Kay, L. E. *J. Mol. Biol.* **1996**, *263*, 369.
(153) Kovrigin, E. L.; Cole, R.; Loria, J. P. *Biochemistry* **2003**, *42*, 5279.
(154) Mildvan, A. S. *Annu. Rev. Biochem.* **1974**, *43*, 357.
(155) Page, M. I. *Angew. Chem., Int. Ed. Engl.* **1977**, *16*, 449.
(156) Williams, D. H.; Stephens, E.; O'Brien, D. P.; Zhou, M. *Angew. Chem., Int. Ed. Engl.* **2004**, *43*, 6596.
(157) Scrofani, S. D. B.; Chung, J.; Huntley, J. J. A.; Benkovic, S. J.; Wright, P. E.; Dyson, H. J. *Biochemistry* **1999**, *38*, 14507.
(158) Huntley, J. J. A.; Scrofani, S. D. B.; Osborne, M. J.; Wright, P. E.; Dyson, H. J. *Biochemistry* **2000**, *39*, 13356.
(159) Freedberg, D. I.; Ishima, R.; Jacob, J.; Wang, Y. X.; Kustanovich, I.; Louis, J. M.; Torchia, D. A. *Protein Sci.* **2002**, *11*, 221.
(160) Osborne, M. J.; Schnell, J.; Benkovic, S. J.; Dyson, H. J.; Wright, P. E. *Biochemistry* **2001**, *40*, 9846.
(161) Munagala, N.; Basus, V. J.; Wang, C. C. *Biochemistry* **2001**, *40*, 4303.
(162) Zhao, Q. J.; Abeygunawardana, C.; Mildvan, A. S. *Biochemistry* **1996**, *35*, 1525.
(163) Cannon, W. R.; Benkovic, S. J. *J. Biol. Chem.* **1998**, *273*, 26257.
(164) Schutz, C. N.; Warshel, A. *Proteins* **2001**, *44*, 400.
(165) Bruice, T. C. *Acc. Chem. Res.* **2002**, *35*, 139.
(166) Mesecar, A. D.; Stoddard, B. L.; Koshland, D. E., Jr. *Science* **1997**, *277*, 202.
(167) Zhao, Q.; Abeygunawardana, C.; Mildvan, A. S. *Biochemistry* **1996**, *35*, 1525.
(168) Yun, S.; Jang, D. S.; Kim, D. H.; Choi, K. Y.; Lee, H. C. *Biochemistry* **2001**, *40*, 3967.
(169) Shapiro, Y. E.; Sinev, M. A.; Sineva, E. V.; Tugarinov, V.; Meirovitch, E. *Biochemistry* **2000**, *39*, 6634.
(170) Stivers, J. T.; Abeygunawardana, C.; Mildvan, A. S.; Whitman, C. P. *Biochemistry* **1996**, *35*, 16036.
(171) Scheuermann, T. H.; Keeler, C.; Hodsdon, M. E. *Biochemistry* **2004**, *43*, 12198.
(172) Shapiro, Y. E.; Kahana, E.; Tugarinov, V.; Liang, Z.; Freed, J. H.; Meirovitch, E. *Biochemistry* **2002**, *41*, 6271.
(173) Stevens, S. Y.; Sanker, S.; Kent, C.; Zuiderweg, E. R. *Nat. Struct. Biol.* **2001**, *8*, 947.
(174) Kern, D.; Zuiderweg, E. R. *Curr. Opin. Struct. Biol.* **2003**, *13*, 748.
(175) Gunasekaran, K.; Ma, B.; Nussinov, R. *Proteins* **2004**, *57*, 433.
(176) Williams, D. H.; Stephens, E.; Zhou, M. *J. Mol. Biol.* **2003**, *329*, 389.
(177) Williams, D. H.; Zhou, M.; Stephens, E. *J. Mol. Biol.* **2006**, *355*, 760.
(178) Clore, G. M.; Driscoll, P. C.; Wingfield, P. T.; Gronenborn, A. M. *Biochemistry* **1990**, *29*, 7387.
(179) Swift, T. J.; Connick, R. E. *J. Chem. Phys.* **1962**, *37*, 307.
(180) Skrynnikov, N. R.; Dahlquist, F. W.; Kay, L. E. *J. Am. Chem. Soc.* **2002**, *124*, 12352.
(181) Trott, O.; Palmer, A. G., III. *J. Magn. Reson.* **2004**, *170*, 104.
(182) Millet, O.; Loria, J. P.; Kroenke, C. D.; Pons, M.; Palmer, A. G. *J. Am. Chem. Soc.* **2000**, *122*, 2867.
(183) Peng, J. W.; Thanabal, V.; Wagner, G. *J. Magn. Reson.* **1991**, *94*, 82.
(184) Szyperski, T.; Luginbühl, P.; Otting, G.; Güntert, P.; Wüthrich, K. *J. Biomol. NMR* **1993**, *3*, 151.
(185) Akke, M.; Palmer, A. G. *J. Am. Chem. Soc.* **1996**, *118*, 911.
(186) Zinn-Justin, S.; Berthault, P.; Guenneugues, M.; Desvaux, H. *J. Biomol. NMR* **1997**, *10*, 363.
(187) Mulder, F. A.; De Graaf, R. A.; Kaptein, R.; Boelens, R. *J. Magn. Reson.* **1998**, *131*, 351.
(188) Korzhnev, D. M.; Orekhov, V. Y.; Dahlquist, F. W.; Kay, L. E. *J. Biomol. NMR* **2003**, *26*, 39.
(189) Trott, O.; Palmer, A. G. *J Magn. Reson.* **2002**, *154*, 157.
(190) Massi, F.; Johnson, E.; Wang, C.; Rance, M.; Palmer, A. G. *J. Am. Chem. Soc.* **2004**, *126*, 2247.
(191) Loria, J. P.; Rance, M.; Palmer, A. G. *J. Am. Chem. Soc.* **1999**, *121*, 2331.
(192) Tollinger, M.; Skrynnikov, N. R.; Mulder, F. A.; Forman-Kay, J. D.; Kay, L. E. *J Am. Chem. Soc.* **2001**, *123*, 11341.
(193) Orekhov, V. Y.; Korzhnev, D. M.; Kay, L. E. *J. Am. Chem. Soc.* **2004**, *126*, 1886.
(194) Korzhnev, D. M.; Kloiber, K.; Kay, L. E. *J. Am. Chem. Soc.* **2004**, *126*, 7320.
(195) Mulder, F. A.; Skrynnikov, N. R.; Hon, B.; Dahlquist, F. W.; Kay, L. E. *J. Am. Chem. Soc.* **2001**, *123*, 967.
(196) Loria, J. P.; Rance, M.; Palmer, A. G. *J. Biomol. NMR* **1999**, *15*, 151.
(197) Hill, R. B.; Bracken, C.; DeGrado, W. F.; Palmer, A. G. *J. Am. Chem. Soc.* **2000**, *122*, 11610.
(198) Ishima, R.; Baber, J.; Louis, J. M.; Torchia, D. A. *J. Biomol. NMR* **2004**, *29*, 187.
(199) Ishima, R.; Torchia, D. A. *J Biomol. NMR* **2003**, *25*, 243.
(200) Ishima, R.; Wingfield, P. T.; Stahl, S. J.; Kaufman, J. D.; Torchia, D. A. *J. Am. Chem. Soc.* **1998**, *120*, 10534.
(201) Wishart, D. S.; Case, D. A. *Methods Enzymol.* **2001**, *338*, 3.
(202) Xu, X. P.; Case, D. A. *Biopolymers* **2002**, *65*, 408.
(203) Korzhnev, D. M.; Salvatella, X.; Vendruscolo, M.; Di Nardo, A. A.; Davidson, A. R.; Dobson, C. M.; Kay, L. E. *Nature* **2004**, *430*, 586.
(204) Wolf-Watz, M.; Thai, V.; Henzler-Wildman, K.; Hadjipavlou, G.; Eisenmesser, E. Z.; Kern, D. *Nat. Struct. Mol. Biol.* **2004**, *11*, 945.
(205) McElheny, D.; Schnell, J. R.; Lansing, J. C.; Dyson, H. J.; Wright, P. E. *Proc. Natl. Acad. Sci., U.S.A.* **2005**, *102*, 5032.
(206) Beach, H.; Cole, R.; Gill, M. L.; Loria, J. P. *J Am. Chem. Soc.* **2005**, *127*, 9167.
(207) Skrynnikov, N. R.; Mulder, F. A. A.; Hon, B.; Dahlquist, F. W.; Kay, L. E. *J. Am. Chem. Soc.* **2001**, *123*, 4556.
(208) Mulder, F. A.; Hon, B.; Mittermaier, A.; Dahlquist, F. W.; Kay, L. E. *J. Am. Chem. Soc.* **2002**, *124*, 1443.
(209) Eriksson, A. E.; Baase, W. A.; Wozniak, J. A.; Matthews, B. W. *Nature* **1992**, *355*, 371.
(210) Eriksson, A. E.; Baase, W. A.; Zhang, X.-J.; Heinz, D. W.; Blaber, M.; Baldwin, E. P.; Matthews, B. W. *Science* **1992**, *255*, 178.
(211) Matthews, D. A.; Alden, R. A.; Bolin, J. T.; Filman, D. J.; Freer, S. T.; Hamlin, R.; Hol, W. G.; Kisliuk, R. L.; Pastore, E. J.; Plante, L. T.; Xuong, N.; Kraut, J. *J. Biol. Chem.* **1978**, *253*, 6946.
(212) Xu, J. A.; Baase, W. A.; Baldwin, E.; Matthews, B. W. *Protein Sci.* **1998**, *7*, 158.
(213) Xu, J.; Baase, W. A.; Quillin, M. L.; Baldwin, E. P.; Matthews, B. W. *Protein Sci.* **2001**, *10*, 1067.
(214) Zhang, X.; Wozniak, J. A.; Matthews, B. W. *J. Mol. Biol.* **1995**, *250*, 527.
(215) Matthews, B. W. *Adv. Protein Chem.* **1995**, *46*, 249.
(216) Griffey, R. H.; Redfield, A. G.; Loomis, R. E.; Dahlquist, F. W. *Biochemistry* **1985**, *24*, 817.
(217) Eriksson, A. E.; Baase, W. A.; Matthews, B. W. *J. Mol. Biol.* **1993**, *229*, 747.
(218) Mulder, F. A.; Hon, B.; Muhandiram, D. R.; Dahlquist, F. W.; Kay, L. E. *Biochemistry* **2000**, *39*, 12614.
(219) Raines, R. T. *Chem. Rev.* **1998**, *98*, 1045.
(220) Cole, R.; Loria, J. P. *Biochemistry* **2002**, *41*, 6072.
(221) Pickett, S. D.; Sternberg, M. J. E. *J. Mol. Biol.* **1993**, *231*, 825.
(222) Creamer, T. P.; Rose, G. D. *Proc. Natl. Acad. Sci., U.S.A.* **1992**, *89*, 5937.
(223) Berger, C.; Weber-Bornhauser, S.; Eggenberger, J.; Hanes, J.; Pluckthun, A.; Bosshard, H. R. *FEBS Lett.* **1999**, *450*, 149.
(224) Bosshard, H. R. *News Physiol. Sci.* **2001**, *16*, 171.
(225) Dürr, E.; Bosshard, H. R. *Eur. J. Biochem.* **1997**, *249*, 325.
(226) Foote, J.; Milstein, C. *Proc. Natl. Acad. Sci., U.S.A.* **1994**, *91*, 10370.
(227) Leder, L.; Berger, C.; Bornhauser, S.; Wendt, H.; Ackermann, F.; Jelesarov, I.; Bosshard, H. R. *Biochemistry* **1995**, *34*, 16509.
(228) Ma, B. Y.; Shatsky, M.; Wolfson, H. J.; Nussinov, R. *Protein Sci.* **2002**, *11*, 184.
(229) Tsai, C. J.; Ma, B.; Sham, Y. Y.; Kumar, S.; Nussinov, R. *Proteins* **2001**, *44*, 418.
(230) Kovrigin, E. L.; Loria, J. P. *Biochemistry* **2006**, *45*, 2636.
(231) Schultz, L. W.; Quirk, D. J.; Raines, R. T. *Biochemistry* **1998**, *37*, 8886.
(232) Monod, J.; Wyman, J.; Changeux, J.-P. *J. Mol. Biol.* **1965**, *12*, 88.
(233) Hardy, J. A.; Wells, J. A. *Curr. Opin. Struct. Biol.* **2004**, *14*, 706.
(234) Kohl, A.; Amstutz, P.; Parizek, P.; Binz, H. K.; Briand, C.; Capitani, G.; Forrer, P.; Pluckthun, A.; Grutter, M. G. *Structure (Cambridge)* **2005**, *13*, 1131.
(235) Verkhivker, G. M.; Bouzida, D.; Gehlhaar, D. K.; Rejto, P. A.; Freer, S. T.; Rose, P. W. *Curr. Opin. Struct. Biol.* **2002**, *12*, 197.

(236) Hitchings, G. H.; Burchall, J. J. *Adv. Enzymol. Relat. Areas Mol. Biol.* **1965**, *27*, 417.
(237) Huennekens, F. M. *Protein Sci.* **1996**, *5*, 1201.
(238) Roth, B.; Cheng, C. C. *Prog. Med. Chem.* **1982**, *19*, 269.
(239) Fierke, C. A.; Johnson, K. A.; Benkovic, S. J. *Biochemistry* **1987**, *26*, 4085.
(240) Miller, G. P.; Benkovic, S. J. *Biochemistry* **1998**, *37*, 6327.
(241) Cameron, C. E.; Benkovic, S. J. *Biochemistry* **1997**, *36*, 15792.
(242) Miller, G. P.; Wahnon, D. C.; Benkovic, S. J. *Biochemistry* **2001**, *40*, 867.
(243) Miller, G. P.; Benkovic, S. J. *Biochemistry* **1998**, *37*, 6336.
(244) Reyes, V. M.; Sawaya, M. R.; Brown, K. A.; Kraut, J. *Biochemistry* **1995**, *34*, 2710.
(245) Sawaya, M. R.; Kraut, J. *Biochemistry* **1997**, *36*, 586.
(246) Venkitakrishnan, R. P.; Zaborowski, E.; McElheny, D.; Benkovic, S. J.; Dyson, H. J.; Wright, P. E. *Biochemistry* **2004**, *43*, 16046.
(247) Falzone, C. J.; Wright, P. E.; Benkovic, S. J. *Biochemistry* **1994**, *33*, 439.
(248) Epstein, D. M.; Benkovic, S. J.; Wright, P. E. *Biochemistry* **1995**, *34*, 11037.
(249) Osborne, M. J.; Venkitakrishnan, R. P.; Dyson, H. J.; Wright, P. E. *Protein Sci.* **2003**, *12*, 2230.
(250) Sikorski, R. S.; Wang, L.; Markham, K. A.; Rajagopalan, P. T.; Benkovic, S. J.; Kohen, A. *J. Am. Chem. Soc.* **2004**, *126*, 4778.
(251) Maglia, G.; Allemann, R. K. *J. Am. Chem. Soc.* **2003**, *125*, 13372.
(252) Swanwick, R. S.; Maglia, G.; Tey, L. H.; Allemann, R. K. *Biochem. J.* **2005**, *394*, 250.
(253) Wang, L.; Tharp, S.; Selzer, T.; Benkovic, S. J.; Kohen, A. *Biochemistry* **2006**, *45*, 1383.
(254) Hammes-Schiffer, S. *Acc. Chem. Res.* **2006**, *39*, 93.
(255) Wu, Y.; Houk, K. N. *J. Am. Chem. Soc.* **1987**, *109*, 906.
(256) Liang, Z. X.; Lee, T.; Resing, K. A.; Ahn, N. G.; Klinman, J. P. *Proc. Natl. Acad. Sci., U.S.A.* **2004**, *101*, 9556.
(257) Adams, J. A.; Fierke, C. A.; Benkovic, S. J. *Biochemistry* **1991**, *30*, 11046.
(258) Liang, Z. X.; Klinman, J. P. *Curr. Opin. Struct. Biol.* **2004**, *14*, 648.
(259) Radkiewicz, J. L.; Brooks, C. L. *J. Am. Chem. Soc.* **2000**, *122*, 225.
(260) Thorpe, I. F.; Brooks, C. L., III. *J Am. Chem. Soc.* **2005**, *127*, 12997.
(261) Rod, T. H.; Radkiewicz, J. L.; Brooks, C. L. *Proc. Natl. Acad. Sci., U.S.A.* **2003**, *100*, 6980.
(262) Thorpe, I. F.; Brooks, C. L. *Proteins* **2004**, *57*, 444.
(263) Watney, J. B.; Agarwal, P. K.; Hammes-Schiffer, S. *J. Am. Chem. Soc.* **2003**, *125*, 3745.
(264) Wong, K. F.; Selzer, T.; Benkovic, S. J.; Hammes-Schiffer, S. *Proc. Natl. Acad. Sci., U.S.A.* **2005**, *102*, 6807.
(265) Agarwal, P. K.; Billeter, S. R.; Rajagopalan, P. T. R.; Benkovic, S. J.; Hammes-Schiffer, S. *Proc. Natl. Acad. Sci., U.S.A.* **2002**, *99*, 2794.
(266) Agarwal, P. K.; Billeter, S. R.; Hammes-Schiffer, S. *J. Phys. Chem. B* **2002**, *106*, 3283.
(267) Kohl, N. E.; Emini, E. A.; Schleif, W. A.; Davis, L. J.; Heimbach, J. C.; Dixon, R. A.; Scolnick, E. M.; Sigal, I. S. *Proc. Natl. Acad. Sci., U.S.A.* **1988**, *85*, 4686.
(268) Seelmeier, S.; Schmidt, H.; Turk, V.; von der, H. K. *Proc. Natl. Acad. Sci., U.S.A.* **1988**, *85*, 6612.
(269) Wlodawer, A.; Vondrasek, J. *Annu. Rev. Biophys. Biomol. Struct.* **1998**, *27*, 249.
(270) Lebon, F.; Ledecq, M. *Curr. Med. Chem.* **2000**, *7*, 455.
(271) Kurup, A.; Mekapati, S. B.; Garg, R.; Hansch, C. *Curr. Med. Chem.* **2003**, *10*, 1679.
(272) Piana, S.; Carloni, P.; Rothlisberger, U. *Protein Sci.* **2002**, *11*, 2393.
(273) Piana, S.; Carloni, P.; Parrinello, M. *J. Mol. Biol.* **2002**, *319*, 567.
(274) Luo, X.; Kato, R.; Collins, J. R. *J. Am. Chem. Soc.* **1998**, *120*, 12410.
(275) Ringhofer, S.; Kallen, J.; Dutzler, R.; Billich, A.; Visser, A. J.; Scholz, D.; Steinhauser, O.; Schreiber, H.; Auer, M.; Kungl, A. J. *J. Mol. Biol.* **1999**, *286*, 1147.
(276) Scott, W. R.; Schiffer, C. A. *Structure* **2000**, *8*, 1259.
(277) Rick, S. W.; Erickson, J. W.; Burt, S. K. *Proteins* **1998**, *32*, 7.
(278) Pillai, B.; Kannan, K. K.; Hosur, M. V. *Proteins* **2001**, *43*, 57.
(279) Lapatto, R.; Blundell, T.; Hemmings, A.; Overington, J.; Wilderspin, A.; Wood, S.; Merson, J. R.; Whittle, P. J.; Danley, D. E.; Geoghegan, K. F. *Nature* **1989**, *342*, 299.
(280) Wlodawer, A.; Miller, M.; Jaskolski, M.; Sathyanarayana, B. K.; Baldwin, E.; Weber, I. T.; Selk, L. M.; Clawson, L.; Schneider, J.; Kent, S. B. *Science* **1989**, *245*, 616.
(281) Spinelli, S.; Liu, Q. Z.; Alzari, P. M.; Hirel, P. H.; Poljak, R. J. *Biochimie* **1991**, *73*, 1391.
(282) Nicholson, L. K.; Yamazaki, T.; Torchia, D. A.; Grzesiek, S.; Bax, A.; Stahl, S. J.; Kaufman, J. D.; Wingfield, P. T.; Lam, P. Y. S.; Jadhav, P. K.; Hodge, C. N.; Domaille, P. J.; Chang, C.-H. *Nat. Struct. Biol.* **1995**, *2*, 274.
(283) Tjandra, N.; Wingfield, P.; Stahl, S.; Bax, A. *J. Biomol. NMR* **1996**, *8*, 273.
(284) Freedberg, D. I.; Wang, Y. X.; Stahl, S. J.; Kaufman, J. D.; Wingfield, P. T.; Kiso, Y.; Torchia, D. A. *J. Am. Chem. Soc.* **1998**, *120*, 7916.
(285) Ishima, R.; Freedberg, D. I.; Wang, Y. X.; Louis, J. M.; Torchia, D. A. *Struct. Fold. Des.* **1999**, *7*, 1047.
(286) Ishima, R.; Louis, J. M.; Torchia, D. A. *J. Mol. Biol.* **2001**, *305*, 515.
(287) Ishima, R.; Petkova, A. P.; Louis, J. M.; Torchia, D. A. *J. Am. Chem. Soc.* **2001**, *123*, 6164.
(288) Nunez, S.; Antoniou, D.; Schramm, V. L.; Schwartz, S. D. *J Am. Chem. Soc.* **2004**, *126*, 15720.
(289) Agarwal, P. K.; Geist, A.; Gorin, A. *Biochemistry* **2004**, *43*, 10605.
(290) Gothel, S. F.; Marahiel, M. A. *Cell. Mol. Life Sci.* **1999**, *55*, 423.
(291) Rovira, P.; Mascarell, L.; Truffa-Bachi, P. *Curr. Med. Chem.* **2000**, *7*, 673.
(292) Handschumacher, R. E.; Harding, M. W.; Rice, J.; Drugge, R. J.; Speicher, D. W. *Science* **1984**, *226*, 544.
(293) Bosco, D. A.; Eisenmesser, E. Z.; Pochapsky, S.; Sundquist, W. I.; Kern, D. *Proc. Natl. Acad. Sci., U.S.A.* **2002**, *99*, 5247.
(294) Eisenmesser, E. Z.; Bosco, D. A.; Akke, M.; Kern, D. *Science* **2002**, *295*, 1520.
(295) Zydowsky, L. D.; Etzkorn, F. A.; Chang, H. Y.; Ferguson, S. B.; Stolz, L. A.; Ho, S. I.; Walsh, C. T. *Protein Sci.* **1992**, *1*, 1092.
(296) Zhao, Y.; Ke, H. *Biochemistry* **1996**, *35*, 7362.
(297) Zhao, Y.; Chen, Y.; Schutkowski, M.; Fischer, G.; Ke, H. *Structure* **1997**, *5*, 139.
(298) Agarwal, P. K. *J Am. Chem. Soc.* **2005**, *127*, 15248.
(299) Haddad, K. C.; Sudmeier, J. L.; Bachovchin, D. A.; Bachovchin, W. W. *Proc. Natl. Acad. Sci., U.S.A.* **2005**, *102*, 1006.
(300) Maciejewski, M. W.; Liu, D. J.; Prasad, R.; Wilson, S. H.; Mullen, G. P. *J. Mol. Biol.* **2000**, *296*, 229.
(301) Akerud, T.; Thulin, E.; Van Etten, R. L.; Akke, M. *J. Mol. Biol.* **2002**, *322*, 137.
(302) Wang, L.; Pang, Y.; Holder, T.; Brender, J. R.; Kurochkin, A. V.; Zuiderweg, E. R. P. *Proc. Natl. Acad. Sci., U.S.A.* **2001**, *98*, 7684.
(303) Huang, Y. T.; Liaw, Y. C.; Gorbatyuk, V. Y.; Huang, T. H. *J. Mol. Biol.* **2001**, *307*, 1075.
(304) Eisenmesser, E. Z.; Millet, O.; Labeikovsky, W.; Korzhnev, D. M.; Wolf-Watz, M.; Bosco, D. A.; Skalicky, J. J.; Kay, L. E.; Kern, D. *Nature* **2005**, *438*, 117.
(305) Van Rompay, A. R.; Johansson, M.; Karlsson, A. *Pharmacol. Ther.* **2000**, *87*, 189.
(306) Vonrhein, C.; Schlauderer, G. J.; Schulz, G. E. *Structure* **1995**, *3*, 483.
(307) Muller, C. W.; Schlauderer, G. J.; Reinstein, J.; Schulz, G. E. *Structure* **1996**, *4*, 147.
(308) Miron, S.; Munier-Lehmann, H.; Craescu, C. T. *Biochemistry* **2004**, *43*, 67.
(309) Rozovsky, S.; Jogl, G.; Tong, L.; McDermott, A. E. *J. Mol. Biol.* **2001**, *310*, 271.
(310) Rozovsky, S.; McDermott, A. E. *J. Mol. Biol.* **2001**, *310*, 259.
(311) Wang, G. P.; Cahill, S. M.; Liu, X.; Girvin, M. E.; Grubmeyer, C. *Biochemistry* **1999**, *38*, 284.
(312) Szilagyi, A.; Zavodszky, P. *Structure* **2000**, *8*, 493.
(313) Akke, M. *Nat. Struct. Mol. Biol.* **2004**, *11*, 912.
(314) Jaenicke, R. *Proc. Natl. Acad. Sci., U.S.A.* **2000**, *97*, 2962.
(315) Jaenicke, R.; Bohm, G. *Curr. Opin. Struct. Biol.* **1998**, *8*, 738.
(316) Kumar, S.; Nussinov, R. *Cell. Mol. Life Sci.* **2001**, *58*, 1216.
(317) Butterwick, J. A.; Loria, J. P.; Astrof, N. S.; Kroenke, C. D.; Cole, R.; Rance, M.; Palmer, A. G. *J. Mol. Biol.* **2004**, *339*, 855.
(318) Mandel, A. M.; Akke, M.; Palmer, A. G. *J. Mol. Biol.* **1995**, *246*, 144.
(319) Feller, G.; Gerday, C. *Cell. Mol. Life Sci.* **1997**, *53*, 830.
(320) Mulder, F. A.; Schipper, D.; Bott, R.; Boelens, R. *J. Mol. Biol.* **1999**, *292*, 111.
(321) Schiraldi, C.; De Rosa, M. *Trends Biotechnol.* **2002**, *20*, 515.
(322) Demirjian, D. C.; Moris-Varas, F.; Cassidy, C. S. *Curr. Opin. Chem. Biol.* **2001**, *5*, 144.
(323) Arora, A.; Abildgaard, F.; Bushweller, J. H.; Tamm, L. K. *Nat. Struct. Biol.* **2001**, *8*, 334.
(324) Salzmann, M.; Pervushin, K.; Wider, G.; Senn, H.; Wüthrich, K. *J. Am. Chem. Soc.* **2000**, *122*, 7543.
(325) Fernandez, C.; Adeishvili, K.; Wuthrich, K. *Proc. Natl. Acad. Sci., U.S.A.* **2001**, *98*, 2358.
(326) Hwang, P. M.; Choy, W. Y.; Lo, E. I.; Chen, L.; Forman-Kay, J. D.; Raetz, C. R.; Prive, G. G.; Bishop, R. E.; Kay, L. E. *Proc. Natl. Acad. Sci., U.S.A.* **2002**, *99*, 13560.
(327) Tugarinov, V.; Kay, L. E. *Biochemistry* **2005**, *44*, 15970.
(328) Howard, B. R.; Endrizzi, J. A.; Remington, S. J. *Biochemistry* **2000**, *39*, 3156.
(329) Anstrom, D. M.; Kallio, K.; Remington, S. J. *Protein Sci.* **2003**, *12*, 1822.
(330) Tugarinov, V.; Choy, W. Y.; Orekhov, V. Y.; Kay, L. E. *Proc. Natl. Acad. Sci., U.S.A.* **2005**, *102*, 622.

(331) Korzhnev, D. M.; Kloiber, K.; Kanelis, V.; Tugarinov, V.; Kay, L. E. *J. Am. Chem. Soc.* **2004**, *126*, 3964.
(332) Tugarinov, V.; Kay, L. E. *J. Mol. Biol.* **2003**, *327*, 1121.
(333) Hwang, P. M.; Bishop, R. E.; Kay, L. E. *Proc. Natl. Acad. Sci., U.S.A.* **2004**, *101*, 9618.
(334) Wang, J.; Hartling, J. A.; Flanagan, J. M. *Cell* **1997**, *91*, 447.
(335) Ortega, J.; Singh, S. K.; Ishikawa, T.; Maurizi, M. R.; Steven, A. C. *Mol. Cell* **2000**, *6*, 1515.
(336) Sauer, R. T.; Bolon, D. N.; Burton, B. M.; Burton, R. E.; Flynn, J. M.; Grant, R. A.; Hersch, G. L.; Joshi, S. A.; Kenniston, J. A.; Levchenko, I.; Neher, S. B.; Oakes, E. S.; Siddiqui, S. M.; Wah, D. A.; Baker, T. A. *Cell* **2004**, *119*, 9.
(337) Huang, X.; Holden, H. M.; Raushel, F. M. *Annu. Rev. Biochem.* **2001**, *70*, 149.
(338) Perham, R. N. *Annu. Rev. Biochem.* **2000**, *69*, 961.
(339) Xu, R.; Ayers, B.; Cowburn, D.; Muir, T. W. *Proc. Natl. Acad. Sci., U.S.A.* **1999**, *96*, 388.
(340) David, R.; Richter, M. P.; Beck-Sickinger, A. G. *Eur. J. Biochem.* **2004**, *271*, 663.
(341) Zuger, S.; Iwai, H. *Nat. Biotechnol.* **2005**, *23*, 736.
(342) Yagi, H.; Tsujimoto, T.; Yamazaki, T.; Yoshida, M.; Akutsu, H. *J. Am. Chem. Soc.* **2004**, *126*, 16632.
(343) Koshland, D. E. *Proc. Natl. Acad. Sci., U.S.A.* **1958**, *44*, 98.
(344) Sinha, N.; Nussinov, R. *Proc. Natl. Acad. Sci., U.S.A.* **2001**, *98*, 3139.
(345) Xue, Q.; Young, E. S. *Nature* **1995**, *373*, 681.
(346) Lu, H. P.; Xun, L.; Xie, X. S. *Science* **1998**, *282*, 1877.
(347) Shi, J.; Palfey, B. A.; Dertouzos, J.; Jensen, K. F.; Gafni, A.; Steel, D. *J. Am. Chem. Soc.* **2004**, *126*, 6914.
(348) Zhang, Z.; Rajagopalan, P. T.; Selzer, T.; Benkovic, S. J.; Hammes, G. G. *Proc. Natl. Acad. Sci., U.S.A.* **2004**, *101*, 2764.
(349) Antikainen, N. M.; Smiley, R. D.; Benkovic, S. J.; Hammes, G. G. *Biochemistry* **2005**, *44*, 16835.
(350) Flomenbom, O.; Velonia, K.; Loos, D.; Masuo, S.; Cotlet, M.; Engelborghs, Y.; Hofkens, J.; Rowan, A. E.; Nolte, R. J.; Van der Auweraer, M.; de Schryver, F. C.; Klafter, J. *Proc. Natl. Acad. Sci., U.S.A.* **2005**, *102*, 2368.
(351) Lerch, H. P.; Rigler, R.; Mikhailov, A. S. *Proc. Natl. Acad. Sci., U.S.A.* **2005**, *102*, 10807.
(352) Min, W.; English, B. P.; Luo, G.; Cherayil, B. J.; Kou, S. C.; Xie, X. S. *Acc. Chem. Res.* **2005**, *38*, 923.
(353) English, B. P.; Min, W.; van Oijen, A. M.; Lee, K. T.; Luo, G.; Sun, H.; Cherayil, B. J.; Kou, S. C.; Xie, X. S. *Nat. Chem. Biol.* **2006**, *2*, 87.
(354) Koradi, R.; Billeter, M.; Wüthrich, K. *J. Mol. Graphics* **1996**, *14*, 51.
(355) Fischer, E. *Ber. Dtsch. Chem. Ges.* **1894**, *27*, 2985.

CR050312Q